

Helicopter Drive System Diagnostics Through Multivariate Statistical Process Control¹

Michael L. Mimmagh
Machinery Silencing Department
Naval Surface Warfare Center
Philadelphia, PA
215-897-1672
MimmaghML@nswc.navy.mil

William Hardman and Jonathan Sheaffer
Propulsion and Power Department
Naval Air Warfare Center, Aircraft Division
Patuxent River, MD
301-757-0508, 301-757-0520
HardmanWJ@navair.navy.mil, SheafferJV@navair.navy.mil

Abstract-- The Naval Air Warfare Center has developed a Helicopter Integrated Diagnostic System (HIDS) which performs mechanical diagnostics on a helicopter's drive system. Diagnostic indicators indicative of the mechanical health of the drive system components are derived from vibration data through a combination of statistical and signal processing methods. This paper discusses the application of a multivariate statistical process control technique known as Hotelling's T2 analysis to HIDS diagnostic indicators. Multivariate analysis uses a composite function of multiple quality indicators to produce a single, trendable indicator that characterizes the state of the monitored process. A statistically valid method of creating and adjusting an alarm threshold for the resultant composite indicator is inherent in the method. When applied to mechanical diagnostic indicators from helicopter drive system seeded fault tests, the method produced timely and unambiguous fault identification with a reduced number of false alarms as compared to current diagnostic methods.

TABLE OF CONTENTS

1. INTRODUCTION
2. BACKGROUND
3. METHODOLOGY
4. PHASE 1: APPLICATION
5. PHASE 2: RESULTS
6. CONCLUSION
7. RECOMMENDATIONS

1. INTRODUCTION

The NAWC, in an integrated program team with BF Goodrich Aerospace under DARPA sponsorship, has developed a Helicopter Integrated Diagnostic System (HIDS) which performs mechanical diagnostics on a helicopter's drive system. Narrowband structureborne vibration data from a helicopter drive system is acquired under various operating regimes. Through a combination of statistical and signal processing methods indicators that qualify drive system component specific features of the vibration data are calculated. A diagnosis is then made of

the mechanical condition of the system based on the values of these indicators. Currently this diagnosis is formulated partly through comparison of the values of individual indicators with hard thresholds and with the mean value of indicators calculated on vibration acquisitions from known healthy systems. A composite function of multiple indicators, known as the component condition indicator, is also calculated and compared to warning and alarm thresholds as the final indication of the mechanical soundness of a particular component.

Current diagnostic procedure is based solely on multiple indicators exceeding their individual alarm thresholds simultaneously in the presence of a fault. However, prior to actual threshold exceedance, it is possible to detect multiple indicators approaching the alarm limits as a fault propagates towards failure. Furthermore, relationships exist among the indicators that are violated as the indicator values change with fault propagation. A deviation of multiple indicators from their baseline values, indicator relationship violations, and alarm threshold exceedances act as indicators of a fault, and the combined effects can give early warning of a fault before the indicators exceed their individual alarm threshold.

This report discusses the application of a statistical process control technique known as multivariate analysis to the HIDS data. Multivariate analysis uses a composite function of multiple quality indicators to produce a single, trendable indicator that characterizes the state of the monitored process. The analysis is sensitive to both quality indicator threshold exceedance and relationship violations. A statistically valid method of creating and adjusting an alarm threshold for the resultant indicator is inherent in the method. A methodology has been developed to select HIDS indicators for incorporation into a multivariate analysis method known as Hotelling's T2 analysis. The indicator selection procedure does not require training on a particular fault. This method is applied to the indicators calculated by the existing diagnostic system and does not put additional demands on on-aircraft hardware or software. When applied to a selected subset of mechanical diagnostic indicators from gear crack propagation tests, the method

¹ "U.S. Government work not protected by US copyright 7803-5846-5/00."

produced timely and unambiguous fault identification with a reduced number of false alarms as compared to current diagnostic methods.

2. BACKGROUND

Multivariate Analysis

The simultaneous monitoring of two or more related process quality indicators is common practice in many industries. Multiple indicators are measured which determine the quality of a process or product. Individual indicators can be monitored by plotting their values against upper and lower control limits. The control limits are determined either by known minimum and maximum process values or through estimation based on observations of the values the indicators take when the process is known to be in control. Typically, the process is considered to be in control only if the value of every monitored quality indicator falls within its control limits simultaneously.

Simultaneous monitoring of multiple quality indicators while applying individual control limits to each is misleading, as illustrated by the following bivariate example [1]. Assume that a normal distribution has been developed for two quality indicators based on data collected when a given process was known to be in control. Assume also that process is defined as out of control if the value of either quality indicator exceeds its control limit by varying from the mean of its in-control distribution by plus or minus three standard deviations. For normally distributed data the probability of any observation of an individual indicator exceeding the plus or minus three-sigma limits is 0.0027. Thus, the probability of the data being within its control limits is 0.9973. In other words, if a sample of one of the normally distributed quality indicator falls outside its plus or minus three-sigma control limit, there is an approximately 99.7% chance that process was out of control when the sample was taken. However, the joint probability that both indicators will simultaneously plot outside the control limits when the process is out of control is $(0.9973) \times (0.9973) = 0.99460729$. Thus the probability that both indicators will concur that the process is out of control when it truly is has been reduced to 99.5%. The probability of both indicators plotting out of control simultaneously is less than that of the individual indicators. The use of individual control limits to monitor each indicator individually distorts the simultaneous monitoring of both indicators. This distortion in the process monitoring procedure increases as the number of quality indicators increases.

Statistical process control methods known as multivariate analyses combine the response of multiple process quality indicators into a single, trendable indicator. Creating and monitoring a single statistic based on all process quality variables can compensate for the distortion caused by the

simultaneous monitoring of multiple indicators. Multivariate methods that treat all the data simultaneously can extract information on how all the variables are behaving relative to one another. Adverse events occurring in a process affect not only the magnitude of the variables, but also their relationship to each other. Variable relationship violations occur even before the individual variables deviate sufficiently from their own in-control means as to be considered out of control. Changes in the relationship between process quality variables are difficult to detect by looking only at the magnitude of each variable independently.

A multivariate method based on the chi-squared statistic has been developed for the collective study of multiple process properties. Known as the Hotelling's T2 statistic (T2), it is calculated by the following equation:

$$T^2 = (\chi - \mu)' \Sigma^{-1} (\chi - \mu)$$

The variable χ is a matrix with the number of rows equal to the number of quality indicators observed and columns containing observations of the indicators. The vector μ contains the in-control means of the indicators. The matrix Σ is the in-control covariance matrix of the indicators. The formula is implemented by first assembling a matrix of in-control observations of the desired number of process quality indicators. The in-control mean of each indicator is calculated and the μ vector is assembled. The in-control covariance matrix Σ is then obtained. The covariance matrix is a symmetric matrix, the number of rows and columns equal to the number of indicators observed, that has the variances of the indicators on the diagonal and their pairwise covariance off the diagonal. Once the in-control μ and Σ are established new single observation of the quality indicators form a χ vector. The in-control indicator means are subtracted from the new observation of each quality indicators to form the $(\chi - \mu)$ vector. The above formula is then implemented to produce a scalar value of T2 for the new observation. As the T2 statistic is calculated for each new indicator observation the result can be trended over time.

The initial implementation of the T2 method on historic, in-control process observations is a T2 vector having a chi-square distribution with degrees of freedom equal to the number of variables included in the analysis. When used to monitor process quality variables, an upper control limit for this statistic is selected based on the number of degrees of freedom of the equation and the desired upper probability density of the distribution. For example, a chi-squared distribution with two degrees of freedom has a 0.005 probability of exceeding the value of 10.597. Therefore, by setting an upper control limit of a T2 analysis of two quality indicators at 10.579, there is a 99.5% chance that when an observation of the T2 statistic exceeds that value the

process from which the quality indicators are collected is out of control.

If new observations of the process quality indicators do not vary from their historic means, the value of T2 calculated for the new observation should be less than the upper control limit established for the baseline chi-square distribution. If, however, at least one of the indicators approaches an out of control value, then the probability that the T2 statistic will exceed its upper control limit increases. Furthermore, if the indicators take on values that are counter to their relationship established in the historic data, even though each may be within its individual control limits, the covariance of the new observation of indicators will change sufficiently to cause the T2 statistic to exceed its upper control limit.

Once the T2 statistic is calculated for successive new process observations they can be plotted against the upper control limit. The result is typically called a chi-square control chart. The advantages of this type of multivariate chart are that the time sequence of the data is preserved and that a single number, the value of T2, characterizes the state of the process. In a multivariate analysis of process quality indicators, a T2 value exceeding its upper control limit can be caused by three main situations. The value of a single indicator may be out of control and thus outside the bounds of the process variation established by the historical data. The relationship between two or more variables may contradict that established by the historical data. Finally, a combination of these two situations could exist with some indicators being out of control and others having counter relationships.

There are two distinct phases of multivariate analysis and trending. In Phase 1 historical observations of indicators are analyzed to determine if the process is in control and to estimate the in control parameters of the process. The chi-square control chart is used to test whether the process was in control when the preliminary data was acquired and the estimation of the in-control indicator mean and covariance matrix was computed. Historical observation of process indicators that plot above the upper control limit of the T2 trend should be examined to determine if assignable causes of the out of control signal can be found in the process. The objective of Phase 1 is to obtain an in-control set of observations so that the in-control parameters of the process can be estimated. Phase 2 is the monitoring of the future process. New observations of the quality indicators are incorporated into the T2 formula and the results trended against the selected upper control limit. An exceedance of the limit indicates that the process has deviated in some way from its in-control condition.

Mechanical Diagnostics

Through the Helicopter Integrated Diagnostic System (HIDS) program the US Navy has developed an integrated diagnostic system for its rotary wing aircraft fleet for the purpose of enhancing operational safety and reducing life cycle costs. The system has the ability to predict impending failures of both structural and dynamic drive system components. Once drive system faults have been detected the system can direct on-condition maintenance actions and/or alert the pilot to conditions affecting flight safety. This functionality is based on the system's ability to perform on board drive system vibration diagnostics and flight regime recognition. The system records multiple vibration channels simultaneously and performs shaft, bearing, and gear analysis on board. Flight events and parameters are recorded for use in regime and usage monitoring.

Fault detection validation tests were conducted in a full-scale helicopter transmission test facility (HTTF) which consists of a SH-60 helicopter drive system, including engines, transmission and tail drive system. Mechanical faults were designed and machined into drive system components and the components installed into the HTTF to simulate typical drive system failures. Fleet removed components rejected at overhaul for excessive wear were also tested in the HTTF. The goals of the tests are to evaluate and validate mechanical diagnostic algorithms and correlate their sensitivity to flight regime and mechanical build.

The diagnostics system determines the operational soundness of a mechanical drive system through signal processing and statistical analysis of structureborne vibration. The diagnostic process can be broken down into major steps. Raw vibration data is acquired from accelerometers mounted on the transmission housing. The raw signal is an aggregation of the vibration of multiple rotating drive system elements within the transmission. The locations of the accelerometers are optimized to capture the contribution of certain drive system components. A database of operating frequencies is kept for the drive system components of interest. Such frequencies include rotational harmonics for shafts, tooth mesh frequencies for gears, and ball pass and race frequencies for bearings. This frequency database is used with signal processing methods that identify component specific aspects of the raw vibration signal. The raw signal is averaged in the time domain using a period of one revolution of a particular component. Filters are constructed to pass frequencies from one component and exclude those of others. In these and other ways aspects of the vibration from a specific component are strengthened in the resulting processed signals. Statistical methods are then applied to both the raw and processed vibration signals in order to qualify aspects of the vibration that indicate the health of the drive system. Descriptive statistics such as root mean square, skewness,

and kurtosis characterize the distribution of the vibration signals. The combined signal processing and statistical analysis of drive system vibration acquisitions results in calculated values known as diagnostic indicators. The indicators are designed such that they are sensitive to the changes in vibration that result from the presence of a mechanically degraded component within the drive system.

Once the responsiveness of the diagnostic indicators has been established, the successful detection of a fault depends on determining an appropriate alarm threshold for each indicator. The value of the alarm threshold must be selected such that it is exceeded in the presence of a fault, but normal variations in the baseline data do not trigger a fault alarm. Conditions exist that cause the value of mechanical diagnostic indicators to vary for reasons other than the presence of a fault. Mechanical drive systems typically operate over a range of regimes, from low power idle to maximum speed and/or torque. The raw vibration of the system, and thus the value of the diagnostic indicators, will change with these changing regimes, though the system health remains the same. Subtle mechanical differences between faultless systems, even though each system is of the same design and operating in the same regime, result in detectable changes in the mean of the diagnostic indicators. System to system variation and operating regime effects have been observed in both HTTF and aircraft data. These conditions complicate the selection of appropriate alarm thresholds for individual diagnostic indicators.

The potential exists to incorporate existing HIDS data into the Hotelling's T2 statistical process control method. The resulting T2 analysis would create a single, trendable indicator based on multiple mechanical diagnostic indicators that characterizes the mechanical condition of a specific drive system component. The quantifiable probability distribution of the chi-square statistic on which T2 is based provides a statistically valid method of creating and adjusting an alarm threshold for the analysis. The ability of the method to detect both indicator mean deviations and relationship violations would provide a more timely warning of progressing faults than current diagnostic procedure, which depends on multiple indicators simultaneously exceeding their individual control limits.

Conditions exist which complicate the application of statistical process control methods to mechanical diagnostics. First, estimating the in-control process parameters of indicator mean and covariance is made difficult by the previously discussed sensitivity of diagnostic indicators to mechanical build and operating regime. The drive system can be viewed as a multiple state process. Even though the process is operating normally the raw vibration that is the physical property on which the diagnostic indicators are being calculated changes with the process state. Second, an appropriate set of indicators must

be selected for use in the T2 analysis. There is a potential risk in building a diagnostic system solely around indicators that deviate from their own distribution in the presence of a particular fault. Often an indicator that responds to one fault will respond to others. However, universal responsiveness is not always the case, and there is risk in attempting to diagnose future unknown faults solely with indicators that have responded to past faults through a deviation from their historical means.

The T2 method can be applied in such a way as to account for the unique requirements of mechanical diagnostics. Grouping the diagnostic data by regime reduces the change in indicator means resulting from changes in operating regime. Observations from multiple builds can be incorporated into the historic baseline database so that the estimation of the in-control parameters of the process will reflect the indicator's build to build variability.

A diagnostic procedure can be developed to take advantage of the sensitivity of T2 to violations of the relationships among diagnostic indicators. By identifying indicators that have a strong relationship in the baseline data that is violated in the presence of a fault and incorporating them into a multivariate analysis a diagnosis can be made without depending on individual indicators exceeding their own alarm thresholds. As multiple indicators become elevated and approach their control limits simultaneously in the presence of a fault, the relationships among the indicators are violated. This results in T2 exceeding its upper control limit before any individual indicator exceeds its own limit, providing an early warning of a progressing fault. The successful application of T2 to the HIDS data is executed through the methodology outlined in the following section.

3. METHODOLOGY

A methodology is developed below for the application of Hotelling's T2 method to the HIDS data. The method creates a multivariate diagnostic indicator that identifies the presence of a fault and limits fault misclassification. The effect of diagnostic indicator sensitivity to build and regime is minimized through logical sub-grouping of the historic data. Indicators are selected for analysis based on their strong relationships in the baseline data. Redundant and ill-conditioned indicators are identified and eliminated from analysis. Faults are identified in HTTF gear crack propagation data based on the value of T2 exceeding a mathematically established upper control limit. The methodology is applicable to both HTTF and aircraft data.

In Phase 1 historical observations of diagnostic indicators are analyzed to determine if the process is in control and to estimate the in control parameters of the process. A univariate chi-square analysis is used as a goodness of fit test for individual indicators to test whether they have a

quantifiable distribution in the baseline data. A correlation study is performed and the indicator pairs with strong relationships are selected for analysis. The estimation of the in-control indicator mean and covariance matrix of the selected indicators is then computed.

Phase 1: Historical Data

In order to begin the process of establishing the in-control levels of the diagnostic indicators a database of indicators from known faultless drive systems must be assembled. The data consists of diagnostic indicators calculated for a single drive system component from the raw vibration of a single accelerometer. Similar component specific data is collected from all comparable drive system sources. The baseline data must be assembled in such a way as to account for the sensitivity of the indicators to build and regime. Indicator samples from multiple baseline builds must be included in the database so that the resultant values of indicator mean and covariance are representative of the variation of different drive system builds. To account for the sensitivity of the diagnostic indicators to operating regime, the historical data samples are organized into subgroups based on regime.

Goodness of Fit

The diagnostic indicators incorporated into the analysis must be jointly distributed according to a multivariate normal distribution. A goodness of fit test based on the chi-square statistic is performed on the individual indicators to test for normal distribution. Any indicator that contains a baseline observation that exceeds a probability distribution of 99.5% is to be excluded from the analysis. To test this the chi-square statistic is calculated for the baseline samples of individual variables and compared against the 99.5 percentile upper control limit of the chi-square distribution with a single degree of freedom. Diagnostic indicators that pass the chi-square goodness of fit test have a low build to build variance and a quantifiable distribution within their operating regime. Redundant indicators can now be eliminated and indicators with strong relationships can be identified for use in the multivariate analysis.

Correlation

Dependence is measured by the degree to which two indicators are correlated. Independent indicators have a correlation coefficient of zero. A single diagnostic indicator can be paired with all other indicators and their correlation can be measured. This type of correlation study reveals that the indicator pairs exhibit a range of correlation, from strongly correlated to strongly anti-correlated.

If seeded fault data is available it is possible to study how the relationship between indicators changes in the presence

of a fault. First a correlation study is preformed on baseline data to measure the correlation of each indicator to the others. Then the same study is performed on faulted data and the results compared with the baseline study. A large change between baseline and fault correlation of an indicator pair indicates that a strong relationship in the baseline data was violated in the presence of a fault. Preliminary study results presented in following sections show that indicator pairs that have a high positive correlation (> 0.9) in the baseline data tend to remain correlated in the presence of a fault. Strong positive correlation in both baseline and faulted data indicates redundancy between the diagnostic indicators in the pair. As a result of the general tendency of all indicators to become elevated in the presence of a fault, certain indicator pairs that are anti-correlated (< -0.70) in the baseline data have been observed to become positively correlated in the presence of a fault. This results in a strong violation of their relationship and a signal of the T2 statistic

The tendency of diagnostic indicators to become elevated in the presence of a fault can be used to advantage for selecting diagnostic indicators for analysis in the absence of seeded fault data. Indicator pairs that are strongly anti-correlated can be identified with baseline data alone. An analysis based on indicators selected in this way does not depend on knowing in advance which indicators respond to a particular fault. Different subsets of indicators were selected for evaluation based on either their change in correlation in the presence of a fault or their strong anti-correlation relationship in baseline data alone.

Estimate In-Control Parameters of Process

The mean and covariance matrix of the selected subset of diagnostic indicators can now be calculated using the build and regime based samples of indicators included in the baseline database. Estimating these in-control parameters is straightforward when using data collected from the HTTF, but can become complicated by the mission constraints of aircraft operating in a fleet environment. Unlike a production line where process data can be sampled at regular intervals and in uniform sample size, the availability of aircraft mechanical diagnostic data can be irregular. Certain regimes from a particular aircraft may not be available, or a large amount of data from one regime may be available from only one aircraft. Including samples of indicator that contain different number of observations, or samples from only a limited number of aircraft, can skew the estimation of the in-control parameters of the process. Alternative methods for estimating the covariance matrix exist which yield a more robust estimate the in-control parameters. Implementing these methods would decrease false alarm rates while preserving the responsiveness of the T2 analysis to faults.

Phase 2: New Observations

Phase 2 consists of monitoring future observations of the selected group of diagnostic indicators. The T2 analysis is performed on incoming data using the historical mean and covariance matrix established in Phase 1. An upper control limit for this analysis is selected based on the number of diagnostic indicators used in the T2 equation and a 99.5% upper probability density of the chi-square distribution. A control chart trending new observations of T2 against the upper control limit is used to detect departures from the relationships and/or in-control means of the indicators established in the historical data. Such departures produce a value of the T2 statistic greater than the upper control limit and signal that an adverse event has occurred in the drive system.

4. PHASE 1: APPLICATION

Gear Fault Data

The data presented in this section is from gear root bending fatigue crack propagation tests generated in the HTTF. Hairline notches were machined into the root of a main module input pinion tooth and an intermediate gear box input pinion tooth. In separate tests, the faults were implanted at their respective locations in the drive system and run until failure. The methodology outlined above was applied to the crack propagation data to create the figures presented in Appendix A.

The first data to be examined is from the main module starboard input pinion crack propagation test. Diagnostic indicators from five baseline builds were identified and assembled into the historic database. In order to propagate the fault in a short time period, the pinion was run in a high torque regime for most of the test. The initial investigation was conducted on high torque data only, and the historic database was modified to contain only high torque data. The chi-square goodness of fit test was then performed on the high torque subgroup and all indicators that did not pass were excluded from further analysis. A correlation study was then performed to identify pairs of indicators whose relationship changes in the presence of a fault. The correlation coefficient of all indicator pairs from the baseline data was calculated and compared to the correlation coefficient of the same indicator pairs calculated on the faulted data. The change in correlation of indicator pairs from baseline to fault was calculated and sorted to determine which pairs had the greatest change. The ten pairs of indicators with the greatest change in correlation are presented in Table 1.

The relationships of indicators 108 and 37 with both 92 and 98 are strongly anti-correlated in baseline data and become somewhat correlated in the presence of a fault, resulting in a

large change in correlation. A multivariate analysis was performed on indicators 108, 37, 92, and 98 and is presented in Figure 1 through 3.

Performing the previous study requires examples of both baseline and faulted data. It is desirable to develop a method of selecting indicators for the multivariate analysis that does not depend on examples of faults. A method was pursued based on the results of the initial correlation study and observations of the indicator's performance on faulted data. It is observed that, in general, in the presence of a fault the values of the diagnostic indicators become elevated. As the value of two indicators that are positively correlated rise in the presence of a fault, the individual limits of each indicator may be violated, but their relationship is not. Note that in the above study the indicators that provided the greatest change in their relationship in the presence of a fault were strongly anti-correlated in the baseline data. Due to the fact that values of the indicators tend to become elevated in the presence of a fault, indicators with strong positive correlation in the baseline data tend to remain positively correlated in the presence of a fault. For the same reason, indicators that are strongly negatively correlated in the baseline data become positively correlated as the indicators become elevated in the presence of a fault. This effect results in a strong violation of their relationship that contributes to a T2 fault signal.

This observation was pursued in another correlation study. Using data from the first correlation study, the value of the baseline correlation of all indicator pairs was sorted to determine the pairs with the highest anti-correlation relationship. The results are presented in Table 2.

The relationship of indicator 41 with indicators 96, 47, and 24 are strongly anti-correlated in the baseline data. The multivariate analysis of these four indicators is presented in Figures 4 through 6. While the change in baseline to fault correlation of indicator pair 41-24 and 41-47 are not as high as other indicator pairs, the combination is sufficient to create a strong signal in the presence of a fault. The significance of the successfulness of these indicators in detecting a fault is that the indicator selection process was not based on responsiveness of any indicator to a particular fault.

An additional criterion should be added to the selection process in order to improve the responsiveness of the analysis. As can be seen in the indicator Plots 1 through 4 of the figures that similarities exist among the indicators selected for the analysis. Among the indicators in Figure 1 selected for their change in correlation, Median Filtered GDF and IGDFbIII appear to be highly similar; likewise IR5a Residual pk2pk and IR5c Residual pk2pk. These similarities are illustrated through the high correlation of the indicators outlined in Table 3. Because of this redundancy, a single

indicator from either set would create an indicator pair that would be just as effective identifying the fault as all four indicators. Similarly, from the indicators selected for anti-correlation, indicators 96, 47, and 24 are all highly correlated with each other. Therefore, an analysis pairing indicator 41 with any one of these indicators would be as successful without including the others.

Indicator correlation should be considered when selecting indicator pairs for analysis. Once an indicator pair is selected for its strong anti-correlation, the following pair should be selected based on their anti-correlation and their independence from all other indicators in the analysis.

A similar study was performed on the intermediate gearbox crack propagation data. As with the main module test, the intermediate gearbox was run at high torque for the majority of the investigation. A baseline database was assembled from acquisitions of the intermediate gearbox input sensor from a number of faultless builds. A high torque regime subgroup of the baseline database was created and a goodness of fit test was performed to eliminate indicators with ill-conditioned distributions. A correlation study was performed on the baseline data to identify those indicator pairs with the strongest anti-correlation relationship. The correlation of the indicator pairs and the change in correlation from baseline to fault was calculated. The results of the study are presented in Table 4.

Indicators were again selected for their strong anti-correlation relationship in the baseline data. The relationship between indicator 108 is strongly anti-correlated with indicators 20 and 43 in the baseline data. From previous correlation studies it is known that indicator 20, Detrended Signal Average Peak to Peak, and indicator 43, Signal Average Peak to Peak, are highly correlated and can be considered redundant. From the results of the anti-correlation study listed in Table 4 it can be observed that there is a high correlation between indicators 20 and 43 and indicators 32 and 33. In selecting a subgroup of these indicators for analysis, it is only necessary to include one of the highly correlated indicators. The next indicator that shows a strong anti-correlated relationship with one indicator under consideration and is not highly correlated with the others is indicator number 84. From the results presented in Table 4, indicators 108, 20, 32, and 84 were selected for analysis. The results of the T2 analysis of these indicators are presented in Figure 9.

Bearing Fault Data

Two separate main module starboard input pinion roller bearing faults are presented. A fleet removed input pinion with a large spall on its inner race was installed in the HTTF and tested over a range of torques. The main module pinion crack propagation test previously presented in the

gear fault section resulted in physical damage to the pinion roller bearing, representing a second bearing fault. The methodology outlined above was applied to data from both bearing faults to create the figures presented in Appendix B.

Since the faults presented are from the same bearing, the same baseline data and diagnostic indicators will be used for both analyses. Diagnostic indicators from five baseline builds were identified and assembled into the historic database. The chi-square goodness of fit test was then performed on baseline bearing indicators and all indicators that did not pass were excluded from further analysis. A correlation study was then performed to identify pairs of that were strongly anti-correlated in the baseline data. The ten pairs of bearing indicators with the greatest baseline anti-correlation are presented in Table 5.

As before, indicator correlation should be considered when selecting indicator pairs for analysis. Once an indicator pair is selected for its strong anti-correlation, the following pair should be selected based on their anti-correlation and their independence from all other indicators in the analysis. Table 6 lists the baseline correlation of the bearing indicator pairs outlined above.

Indicator pairs for the bearing analysis were selected for their strong anti-correlation relationships in the baseline data and their independence from subsequently selected indicator pairs. The relationship between indicator 18 is strongly anti-correlated with indicator 19 in the baseline data. From the correlation studies presented in Table 6 it is known that indicator 25 is highly correlated with indicator 19, and indicator 45 is highly correlated with indicator 18; indicators 25 and 45 used in conjunction with 18 and 19 or paired with themselves can be considered redundant. The next indicator pair that shows a strong anti-correlated relationship and is not highly correlated with the others is 22 and 34. From the results presented in Tables 5 and 6, indicators 18, 19, 22, and 34 were selected for initial bearing analysis. An alternate combination of indicators is 18, 19, 16, and 52. While indicator 16 is correlated with 18, the strong anti-correlation of 52 with 16, and therefore 18, should yield good diagnostic performance. The results of the T2 analyses of the starboard main module input pinion roller bearing faults using each set of selected indicators are presented in Figure 11 through 18.

5. PHASE 2: RESULTS

Gear Fault Diagnostics

The developed methodology was applied to the main module and intermediate gearbox baseline and crack propagation data. Correlation studies were used to select indicators for incorporation into the T2 analysis. Indicator groups were selected based on both their change in

correlation in the presence of a fault as well as their high anti-correlation relationship in the baseline data alone. The T2 analysis was performed and the results are presented in Appendix A.

Figure 1 plots the four indicators selected from the change in correlation study listed in Table 1 of the HTTF main module crack propagation data. All of the following analyses are performed using four diagnostic indicators. The upper control limit was selected based on a 99.5% percentile of the chi-square distribution. For an analysis with four degrees of freedom this results in an upper control limit of 14.86, which is applied in Plot 5 of all figures. The data presented in Figure 1 is for all torque levels. The indicators selected from the correlation study are shown in Plots 1 through 4. Acquisitions 1 through 205 are baseline data from three different test cell builds. The remaining acquisitions are the crack propagation test. The fault data is presented in chronological order. A vertical line on each plot separates the baseline from the fault propagation data. Plot 5 is the T2 statistic plotted against its upper control limit. Note the strong response of the T2 statistic as the fault propagates towards failure. Plot 6 is an alarm threshold exceedance plot of the T2 statistic compared with the BFG component condition indicator. When either composite indicator exceeds its upper control limit it is indicated by a step elevation in the signal. A warning and an alarm limit are applied to the BFG indicator. For this analysis T2 exceeds its upper control limit approximately 7 times in the baseline data. The BFG component condition indicator exceeds its warning threshold approximately 16 times in the same region. When either analysis signals in the baseline data it is considered a false alarm.

The test cell main module pinion crack propagation test was run at two torque settings. The majority of acquisitions were at 450 foot-pounds engine torque. This torque is within the maximum torque range that the test cell is capable of generating. Low engine torque data at 150 foot-pounds were also acquired. Figure 2 plots the same four indicators selected from the change in correlation study and plotted in Figure 1; the data presented is for engine torque greater than 400 foot-pounds. Plots 5 and 6 show the strong response of the T2 statistic in the presence of the fault and the elimination of false alarms in the baseline data. There are approximately 6 warnings in the baseline data from the BFG indicator. Figure 3 plots the indicators acquired at low engine torque. The same strong response to the fault is evident in the T2 statistic. Three false alarms occur in the T2 analysis, and seven in the BFG analysis.

Figure 4 plots the four indicators selected from the maximum anti-correlation study listed in Table 2 for the entire range of torque of the main module data. As can be seen in Plots 5 and 6 the performance of these indicators is comparable to those of the first study. Six false alarms occur in the T2

statistic with this indicator combination. Figure 5 plots the same indicators for high torque acquisitions only. The response to the fault is less ambiguous and the false alarms are reduced to one. Figure 6 presents the low torque acquisitions of the selected indicators. This analysis also responds to the fault with reduced false alarms over the BFG analysis.

Figure 7 plots a subset of indicators that pass the chi-square goodness of fit test in both the baseline and fault data of the high torque main module crack propagation test. That is, based on the historic observation of these indicators, any indicator individually would not exceed its own alarm threshold in the presence of the propagating gear fault. The levels of all indicators remain well within their historic baseline distributions for all observations of the fault. However the T2 analysis of these indicators produces a strong indication of the fault with no false alarms, as seen in Plots 5 and 6.

Figure 8 plots the T2 performance of the indicators selected from the main module anti-correlation study on the intermediate gearbox crack propagation data. The intermediate gearbox crack propagation fault was run at high torque only. It can be seen in Plot 3 that the Raw Data Kurtosis indicator for all acquisitions of the fault test build is markedly different from the baseline data. Because of this the initial elevation of the T2 signal may be partially build related, but the eventual and extremely strong response of the statistic illustrated in Plot 5 indicates the success of the selected indicators in detecting the progressing fault.

Figure 9 plots the four indicators selected from the high anti-correlation study listed in Table 4 for the intermediate gearbox crack propagation data. Plots 1 and 3 show the strong response of the selected indicators to the propagating fault. This yields a strong and timely response in the T2 statistic in Plot 5. There are 10 T2 false alarms in the baseline data. There are approximately 24 false alarms from the BFG analysis.

Figure 10 plots performance of the intermediate gearbox indicators selected for high baseline anti-correlation on a one third tooth fault in the intermediate gearbox input pinion. The analysis results in an extremely strong response, as seen in the log scale of Plot 5. The maximum T2 value is 1200, approximately 85 times the upper control limit.

Bearing Fault Diagnostics

The plot format for the bearing analysis is identical to that of the gear analysis. A four degree of freedom T2 upper control limit was selected based on a 99.5% percentile of the chi-square and an upper control limit of 14.86 was applied in Plot 5 of all figures. A vertical line on each plot separates the

baseline from the fault data. Plot 5 is the T2 statistic plotted against its upper control limit. Plot 6 is an alarm threshold exceedance plot of the T2 statistic compared with the BFG component condition indicator.

The first data to be examined is from the main module pinion roller bearing inner race spall test. Data was taken twelve times during the test, with the sample torque ranging from 100 to 410 ft. lbs. Due to the small fault data sample size, all torques were included in the analysis. Figure 11 plots the first selected diagnostic indicator suite. All indicators respond to the fault, which results in a T2 strong signal and no false alarms. Figure 12 plots the second indicator suite used to analyze the fault, which also yields a strong response to the fault.

The second starboard main module input pinion roller bearing fault occurred during a gear crack propagation test. The pinion crack propagated into the inner race of the pinion roller bearing, which is integrated into the pinion. The test was run over a range of torques, and analyses were performed on the entire data set, as well as high and low torque subsets. Figures 13 through 15 are the analysis of the first suite of diagnostic indicators. When all torques are included in the analysis the resultant T2 signal responds well, though it does dip below the alarm threshold for a low torque run in the late stages of the test as seen in Figure 13. The high and low torque regime analyses shown in Figures 14 and 15 show an improvement in T2 performance, with the indicator remaining in alarm. As illustrated in Plot 6 of Figure 15, T2 performance on low torque data is superior to the BFG method, which never achieves alarm levels for this data. Figures 16 through 18 plot the analysis of the integral race crack data using the second suite of selected diagnostic indicators. The performance of these indicators on this fault is not as strong as the first suite, though improvements in diagnostic performance through separate torque analysis is evident.

Discussion

Figures 1 through 3 plot the four indicators selected from the change in correlation study for the main module pinion crack propagation test. It can be seen in Plots 5 and 6 of each figure that the T2 statistic performs well in detecting the presence of the growing gear tooth crack before the fault propagates to failure. Both T2 and the BFG indicator detect the fault in a timely manner, but the strong response of T2 in exceeding its upper control limit provides a more unambiguous indication of the presence of the fault. When performed on data from all torque regimes, there is a 56% reduction in false alarm from current BFG analysis levels. When the data is organized into subgroups based on operating regimes the reduction in false alarms is more pronounced. The low torque regime analysis in Figure 3

yields a 77% reduction in false alarm, and in Figure 2 false alarms are eliminated for the high torque analysis.

Figures 4 through 6 plot the four indicators selected from the maximum anti-correlation study for the main module pinion crack propagation test. Recall that these indicators were not selected for their performance in this particular fault, but solely on their strong relationships in the baseline data. These indicators perform as well in detecting the growing fault and reducing false alarms as those selected in the first study. Similar reductions in number of false alarms are achieved overall and by grouping the analysis by regime. False alarms are reduced to one for the high torque analysis.

Figure 7 illustrates the sensitivity of T2 to changes in relationship among the indicators incorporated into the analysis. Even though none of the indicator would exceed their individual alarm thresholds, the violation of their relationship as the fault progresses causes T2 to signal.

Figure 8 illustrates how the indicators selected for high anti-correlation in the main module baseline data perform on data from the intermediate gearbox. The immediate elevation of the T2 signal in Plot 5 is likely due to the clear difference in Plot 3 of the values of Raw Data Kurtosis from baseline to fault builds. In that the crack is known to have propagated from a small notch, this effect is most likely build related. The build effect alone is not sufficient to cause the T2 analysis to exceed its upper control limit. The baseline data used to estimate the in-control mean and covariance is representative enough to allow for the variation of a new build. As the indicators respond to the propagating fault, the T2 signal becomes extremely strong. Although the two gearboxes contain different drive system components, the analysis shows that the selected indicators perform well in detecting the same type of fault in both the main module and the intermediate gearbox. A 74% reduction in false alarms is illustrated in Plot 6.

Figure 9 plots the indicators selected from the anti-correlation study for the intermediate gearbox crack propagation test data. Again as seen in Plot 5, there is an immediate elevation in the T2 statistic that is most likely build related and insufficient to cause an alarm in the analysis. This elevation is insignificant compared to the response of T2 to the progressing fault. False alarms are reduced by approximately 50%.

Figure 10 plots the performance of the indicators selected from the intermediate gearbox anti-correlation study on the intermediate gearbox 1/3 tooth fault data. In that the tooth fault was severe, the strong response of the T2 analysis is not surprising but, as with Figure 8, it illustrates how indicators that are selected to perform on a particular fault can perform equally well on other types of faults.

Figures 11 and 12 plot two separate suites of indicators used to analyze the starboard main module input pinion roller bearing inner race spall. Indicator pairs in the suites were selected for their anti-correlation relationship. The suites differ in the level of independence of the indicator pairs that constitute the suite. The strong response of the indicators in Plots 2 through 4 of Figure 11 contribute to the T2 signal, which is consistently in alarm for all of the fault data. By comparison, the BFG component indicator oscillates between warning and alarm levels. Figure 12 plots the second indicator suite selected for analysis. While the indicators plotted in Plots 3 and 4 are not as responsive as those in Figure 11, their change in relation in the presence of the fault, coupled with the strong response of the indicator in Plot 2 result in a strong T2 signal. This analysis produced one false alarm. False alarm rates would be improved if this analysis had been performed on acquisitions of torque subgroups.

The analysis of the pinion roller bearing crack fault for the first suite of diagnostic indicators is featured in Figures 13 through 15. Along with the strong performance of T2 in detecting this fault, this analysis illustrates the improvements in diagnostic performance achievable through regime specific analysis. Figure 13 plots the analysis performed on all torques. While the T2 analysis yields a stronger response than the BFG component condition, both drop below warning levels for a low torque data acquisition taken during an advanced stage of fault propagation. The high torque analysis presented in Figure 14 shows the T2 levels consistently above alarm levels towards the end of the fault test, while the BFG indicator oscillates between warning and alarm. The low torque analysis in Figure 15 also shows T2 in alarm for the late stage fault acquisitions, including the sample identified as healthy in the all-torque analysis. One false alarm is visible in Figure 12.

Figures 16 through 18 illustrate the sensitivity of T2 to changes in relationship among the indicators incorporated into the analysis. This analysis was performed on the bearing inner race crack using the second suite of indicators selected through the bearing indicator anti-correlation study. Indicator values in the presence of the fault do not exceed those in the baseline data. However, general indicator elevation and the violation of indicator relationships as the fault progresses cause T2 to signal. The overall response of this analysis is not as strong as that of the first indicator suite.

There are a number of observations that apply to every T2 analysis performed. Organizing the historic data into subgroups based on regime significantly reduced false alarms while maintaining responsiveness to the faults. The response of T2 in the presence of a fault is strong for every analysis. This indicates that more conservative estimates of

the upper control limit or the in-control process characteristics could be used without significantly sacrificing diagnostic performance. The upper control limit could be selected based on a higher percentile of the chi-square distribution, such as 99.99%. This would increase the value of the upper control limit that is applied to both baseline and fault data, reducing false alarms due to baseline outliers while maintaining responsiveness to faults. If desired, a warning limit could be incorporated into the analysis, using a chi-square distribution of 99.50% as a warning limit and 99.99% as an alarm.

6. CONCLUSION

Hotelling's T2 statistical quality control technique has been applied to existing mechanical diagnostic indicators and outperforms current diagnostic methods in detecting mature and propagating drive system faults while reducing fault misclassification. A methodology has been developed for the application of the Hotelling's T2 multivariate statistical process control technique using current US Navy HIDS diagnostic data as process quality indicators. The method does not require training on particular faults and the indicators selected through the methodology are responsive to more than one type of fault. A statistically valid method of selecting an alarm threshold is incorporated into the method. When the methodology is applied to gear crack propagation data it yields a strong, timely, and unambiguous indication of the growing fault and a minimum reduction in false alarms of 50% over current diagnostic procedure. Incorporating regime recognition into the gear fault analysis reduced the number of false alarm by 70%. Hotelling's T2 technique and the methodology used to select indicators for analysis was successful in identifying two types of bearing faults. The analysis yielded a stronger response in the presence of a mature bearing race spall than current diagnostic methods. The method also outperformed current diagnostic methods on a propagating bearing race crack. Regime recognition increased the responsiveness of the T2 statistic to both bearing fault analyses. The response of T2 in the presence of a fault is strong for every analysis. This indicates that more conservative estimates of the upper control limit or the in-control process characteristics could be used, thereby further decreasing the rate of false alarms without significantly sacrificing diagnostic performance.

7. RECOMMENDATIONS

The potential exists to further adapt multivariate statistical process control methods for use with HIDS mechanical diagnostics indicators. Implementation of the following recommendations would yield a component condition indicator with improved response to faults that is less sensitive to normal build to build variations in the historic data, thus reducing false alarm rates.

The T2 statistic responds to indicator mean and relationship violations, and thus its performance is based on the individual indicator's capacity to represent the process being monitored. An individual diagnostic indicator's responsiveness to a particular fault is self evident, but a methodology is required to quantify the change in relationship of one indicator to another in the presence of a propagating fault. In this study diagnostic indicator correlation was used to quantify their relationships. Indicators with strong anti-correlation were selected empirically based on available baseline data. Further study into the mathematics of the calculated indicators should be conducted to reveal the exact nature of their relationships and the reason these relationships change in the presence of a fault. Once the relationship is established the pair of indicators would be able to detect the presence of a fault through the violation of that relationship only, and not through individual indicators exceeding hard thresholds.

Once a suite of diagnostic indicators has been selected for analysis, estimation of the in-control mean and covariance of the indicators becomes the most critical aspect of the analysis. Alternative methods for estimating indicator mean and covariance exist which use the vector differences of successive observations to yield a more robust estimate of the in-control parameters. This may reduce the magnitude of the T2 signal in the presence of a fault, but make the analysis less sensitive to false alarms that might result from new drive system data acquisitions. Subsequent T2 analyses should be performed using the vector differences of successive baseline observations to estimate the in-control parameters of the system.

Additional statistical processing control tools are available and can be incorporated into the current analysis procedures to assist in the interpretation of the T2 signal. **Decomposition** techniques exist that separate the T2 statistic into independent parts that can be evaluated to determine which variable or set of variables is out of control, and whether the out of control signal is a result of a shift in mean of a particular indicator or a relationship violation. These methods identify the cause of the out of control signal without the need to examine the univariate charts of the individual indicators.

The analysis presented in this report was performed using no more than five baseline HTTF configurations as historic data. Incorporating additional historic data into the analysis would create a more representative baseline data sample and improve the diagnostic performance of the analysis. Ultimately the analysis should be tested on aircraft data. Sufficient HIDS data from test aircraft is available to begin assembling historic baseline data and initiate estimates of the in control parameters of the aircraft mechanical drive system.

REFERENCES

- [1] C. A. Lowry, W. H. Woodall, C. W. Champ, S. E. Rigdon, "A multivariate Exponentially Weighted Moving Average Control Chart", *Technometrics*, Vol 34, No. 1, pp. 46-53, 1992.
- [2] D. M. Hawkins, "Regression Adjustment for Variables in Multivariate Quality Control", *Journal of Quality Technology*, Vol. 25, No. 3, pp. 170-182, 1993.
- [3] R. L. Mason, N. D. Tracy, J. C. Young, "Decomposition of T2 for Multivariate Control Chart Interpretation", *Journal of Quality Technology*, Vol. 27, No. 2, pp. 99-108, 1995.
- [4] T. Kourti, J. F. MacGregor, "Multivariate SPC Methods for Process and Product Monitoring", *Journal of Quality Technology*, Vol. 28, No. 4, pp. 409-426, 1996.
- [5] J. H. Sullivan, W. H. Woodall, "A Comparison of Multivariate Control Charts for Individual Observations", *Journal of Quality Technology*, Volume 28, No. 4, pp. 398-407, 1996.
- [6] R. L. Mason, N. D. Tracy, J. C. Young, "A Practical Approach for Interpreting Multivariate T2 Control Chart Signals", *Journal of Quality Technology*, Vol. 29, No. 4, pp. 396-406, 1997.

BIOGRAPHIES

Michael Mimmagh is a Mechanical Engineer for the Machinery Research and Development Directorate, Machinery Silencing Department, of the Naval Surface Warfare Center-Cardero Division in Philadelphia, PA. As an engineer for the Naval Air Warfare Center he performed diagnostic algorithm development and validation and conducted SH-60 drive system seeded fault tests for the Helicopter Integrated Diagnostic System program. In addition he provided mechanical diagnostic support to other aircraft platforms, including the F-18 and the Joint Strike Fighter program. His current research is directed towards submarine silencing under the Office of Naval Research's Quiet Electric Drive program. He holds a BSME and a MSME from Villanova University.



Bill Hardman is a Diagnostics Engineer for the Propulsion and Power Department of the Naval Air Warfare Center, Patuxent River, MD.



He has been working on diagnostic and control system applications for more than ten years. Major projects include the following: lead diagnostics engineer for the Integrated Mechanical Diagnostics Health and Usage Monitoring System,

Helicopter Integrated Diagnostic System (HIDS) researcher on diagnostics algorithms and applications, lead engine control engineer for the F/A-18 F414 engine control system development, and T700 engine control support engineer. He holds a BSME from Temple University and a MSME from Drexel University. Of particular note, Bill has played a key role in developing novel techniques for bearing fault detection and is regarded as the Navy expert in drive system diagnostics.

Jonathan V. Sheaffer is a graduate of The Pennsylvania State University, with a BS in Aerospace Engineering and a minor in Engineering Mechanics. Upon graduation he obtained a position working for the Propulsion and Power Department of the Naval Air Warfare Center, Patuxent River, MD as a Diagnostics and Controls Engineer. Major projects include the following: T58 engine control system, Integrated Mechanical Diagnostics Health and Usage Monitoring System, and Helicopter Integrated Diagnostics System (HIDS) Flight Testing/Development Support for the CH-53, SH-60 and H-1 aircraft. Other project areas are the support of various programs to enhance current diagnostic/prognostic capabilities, including work with some international organizations. He is currently working toward a FAA sanctioned Private Pilot's License.

Table 1. Main Module Starboard Input Pinion Indicator Pairs from Starboard Main Accelerometer Sorted by Change in Correlation from Baseline to Fault.

Indicator 1 Number & Name	Indicator 2 Number & Name	Baseline Correlation	Faulted Correlation	Correlation Change
108 median filtered GDF (ND)	92 IR5a Residual pk2pk (G)	-0.850	0.527	1.377
108 median filtered GDF (ND)	98 IR5c Residual pk2pk (G)	-0.836	0.537	1.374
92 IR5a Residual pk2pk (G)	37 IGDFbIII (ND)	-0.778	0.579	1.357
98 IR5c Residual pk2pk (G)	37 IGDFbIII (ND)	-0.767	0.588	1.355
92 IR5a Residual pk2pk (G)	34 IGDFaII (ND)	-0.774	0.581	1.354
92 IR5a Residual pk2pk (G)	35 IGDFbII (ND)	-0.774	0.581	1.354
98 IR5c Residual pk2pk (G)	34 IGDFaII (ND)	-0.757	0.589	1.346
98 IR5c Residual pk2pk (G)	35 IGDFbII (ND)	-0.757	0.589	1.346
92 IR5a Residual pk2pk (G)	36 IGDFaIII (ND)	-0.754	0.578	1.332
98 IR5c Residual pk2pk (G)	36 IGDFaIII (ND)	-0.727	0.587	1.314

Table 2. Main Module Starboard Input Pinion Indicator Pairs from Starboard Main Accelerometer Sorted by Ascending Baseline Correlation.

Indicator 1 Number & Name	Indicator 2 Number & Name	Baseline Correlation	Faulted Correlation	Correlation Change
96 IR1a Residual RMS (G)	41 RAW DATA kurtosis (ND)	-0.916	0.000	0.916
24 DT SIG AVG RMS (G)	41 RAW DATA kurtosis (ND)	-0.911	-0.679	0.232
41 RAW DATA kurtosis (ND)	47 SIG AVG RMS (G)	-0.905	-0.679	0.226
102 IR1c Residual RMS (G)	41 RAW DATA kurtosis (ND)	-0.904	0.002	0.906
18 RAW DATA 6M (ND)	96 IR1a Residual RMS (G)	-0.896	0.056	0.951
41 RAW DATA kurtosis (ND)	109 median filtered RTE	-0.895	-0.717	0.179
24 DT SIG AVG RMS (G)	37 IGDFbIII (ND)	-0.892	-0.379	0.513
37 IGDFbIII (ND)	47 SIG AVG RMS (G)	-0.891	-0.379	0.512
108 median filtered GDF (ND)	96 IR1a Residual RMS (G)	-0.890	0.356	1.246
20 DT SIG AVG pk2pk (G)	41 RAW DATA kurtosis (ND)	-0.890	-0.210	0.680

Table 3. Gear Indicator Pair Correlation.

Indicator 1 Number & Name	Indicator 2 Number & Name	Baseline Correlation	Faulted Correlation	Correlation Change
47 SIG AVG RMS (G)	24 DT SIG AVG RMS (G)	0.998	1.000	0.002
96 IR1a Residual RMS (G)	24 DT SIG AVG RMS (G)	0.947	0.646	0.301
96 IR1a Residual RMS (G)	47 SIG AVG RMS (G)	0.947	0.646	0.301
108 median filtered GDF (ND)	37 IGDFbIII (ND)	0.925	0.902	0.023
92 IR5a Residual pk2pk (G)	98 IR5c Residual pk2pk (G)	0.991	0.998	0.007

Table 4. Intermediate Gearbox Pinion Indicator Pairs from Intermediate Gearbox Input Accelerometer Sorted by Ascending Baseline Correlation.

Indicator 1 Number & Name	Indicator 2 Number & Name	Baseline Correlation	Faulted Correlation	Correlation Change
108 IGBInpt median filtered GDF	20 IGBInpt DT SIG AVG pk2pk	-0.734	0.768	1.502
108 IGBInpt median filtered GDF	43 IGBInpt SIG AVG pk2pk	-0.733	0.769	1.501
20 IGBInpt DT SIG AVG pk2pk (G)	32 IGBInpt IGDFa (ND)	-0.721	0.940	1.661
20 IGBInpt DT SIG AVG pk2pk (G)	33 IGBInpt IGDFbII (ND)	-0.721	0.940	1.661
32 IGBInpt IGDFa (ND)	43 IGBInpt SIG AVG pk2pk (G)	-0.717	0.941	1.658
33 IGBInpt IGDFbII (ND)	43 IGBInpt SIG AVG pk2pk (G)	-0.717	0.941	1.658
32 IGBInpt IGDFa (ND)	84 IGBInpt EO RMS (G)	-0.716	0.863	1.579
33 IGBInpt IGDFbII (ND)	84 IGBInpt EO RMS (G)	-0.716	0.863	1.579
108 IGBInpt median filtered GDF	68 IGBInpt raw base energy RMS	-0.715	0.634	1.349
29 IGBInpt Narrowband pk2pkNB5	61 IGBInpt G2(1) (ND)	-0.714	0.978	1.692

Table 5. Main Module Starboard Input Pinion Roller Bearing Indicator Pairs from Starboard Main Accelerometer Sorted by Ascending Baseline Correlation.

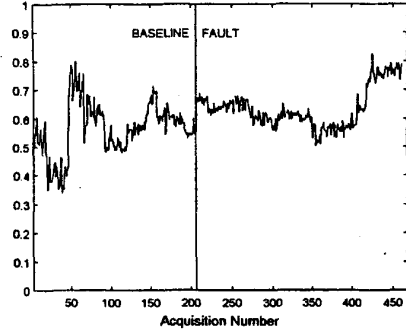
Indicator 1 Number & Name	Indicator 2 Number & Name	Baseline Correlation	Faulted Correlation	Correlation Change
18 StbdMain Raw Kurtosis	19 StbdMain Raw RMS	-0.868	-0.424	0.444
18 StbdMain Raw Kurtosis	25 StbdMain Raw Tone Energy	-0.862	-0.425	0.437
19 StbdMain Raw RMS	45 StbdMain Raw Data 6M	-0.843	-0.496	0.347
25 StbdMain Raw Tone Energy	45 StbdMain Raw Data 6M	-0.836	-0.497	0.339
16 StbdMain Raw Crest Factor	19 StbdMain Raw RMS	-0.819	-0.778	0.041
45 StbdMain Raw Data 6M	52 StbdMain TSBC	-0.818	0.235	1.053
16 StbdMain Raw Crest Factor	25 StbdMain Raw Tone Energy	-0.816	-0.78	0.035
22 StbdMain Enveloped Skewness	34 StbdMain Number of Peaks	-0.816	0.654	1.471
34 StbdMain Number of Peaks	38 StbdMain Bearing Health Index	-0.802	0.293	1.095
18 StbdMain Raw Kurtosis	52 StbdMain TSBC	-0.799	0.181	0.980

Table 6. Bearing Indicator Pair Correlation

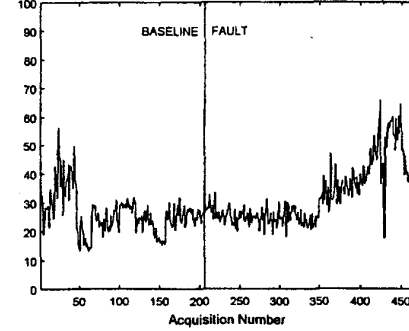
Indicator 1 Number & Name	Indicator 2 Number & Name	Baseline Correlation	Faulted Correlation	Correlation Change
19 StbdMain Raw RMS	25 StbdMain Raw Tone Energy	0.999	1.000	0.001
18 StbdMain Raw Kurtosis	45 StbdMain Raw Data 6M	0.996	0.983	0.012
22 StbdMain Enveloped Skewness	38 StbdMain Bearing Health Index	0.849	-0.101	0.950
19 StbdMain Raw RMS	52 StbdMain TSBC	0.749	-0.654	1.403
16 StbdMain Raw Crest Factor	18 StbdMain Raw Kurtosis	0.727	0.552	0.374
18 StbdMain Raw Kurtosis	34 StbdMain Number of Peaks	0.178	0.046	0.132
19 StbdMain Raw RMS	34 StbdMain Number of Peaks	0.091	-0.715	0.806
19 StbdMain Raw RMS	22 StbdMain Enveloped Skewness	-0.070	-0.732	0.662
18 StbdMain Raw Kurtosis	22 StbdMain Enveloped Skewness	-0.270	0.036	0.306

Appendix A: Results of T2 Gear Analysis

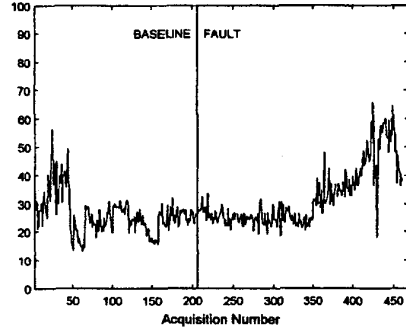
Plot #1: StbdMainPin-StbdMain median filtered GDF (ND)



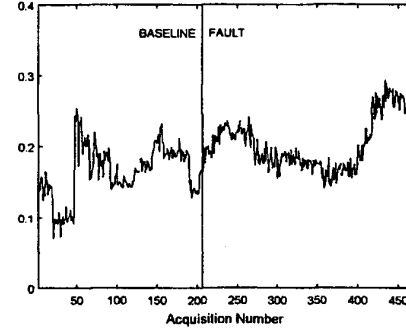
Plot #2: StbdMainPin-StbdMain IR5a Residual pk2pk (G)



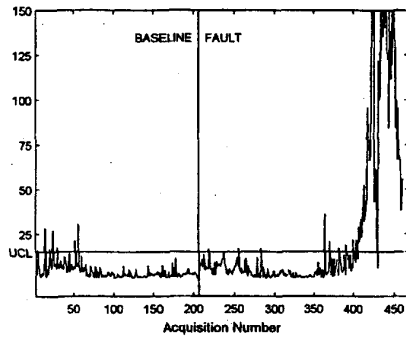
Plot #3: StbdMainPin-StbdMain IR5c Residual pk2pk (G)



Plot #4: StbdMainPin-StbdMain IGDFbIII (ND)



Plot #5: T2



Plot #6: Component Condition

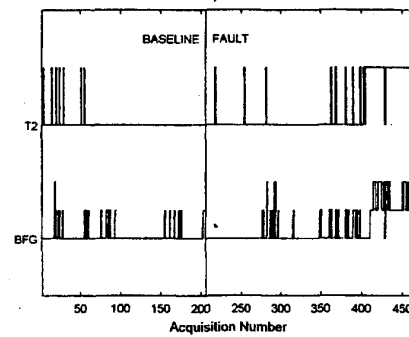


Figure 1. Main Module Starboard Input Pinion Crack Propagation Data: All Torque Indicators Selected from Starboard Main Accelerometer for Max Indicator Δ Correlation from Baseline to Fault Data.

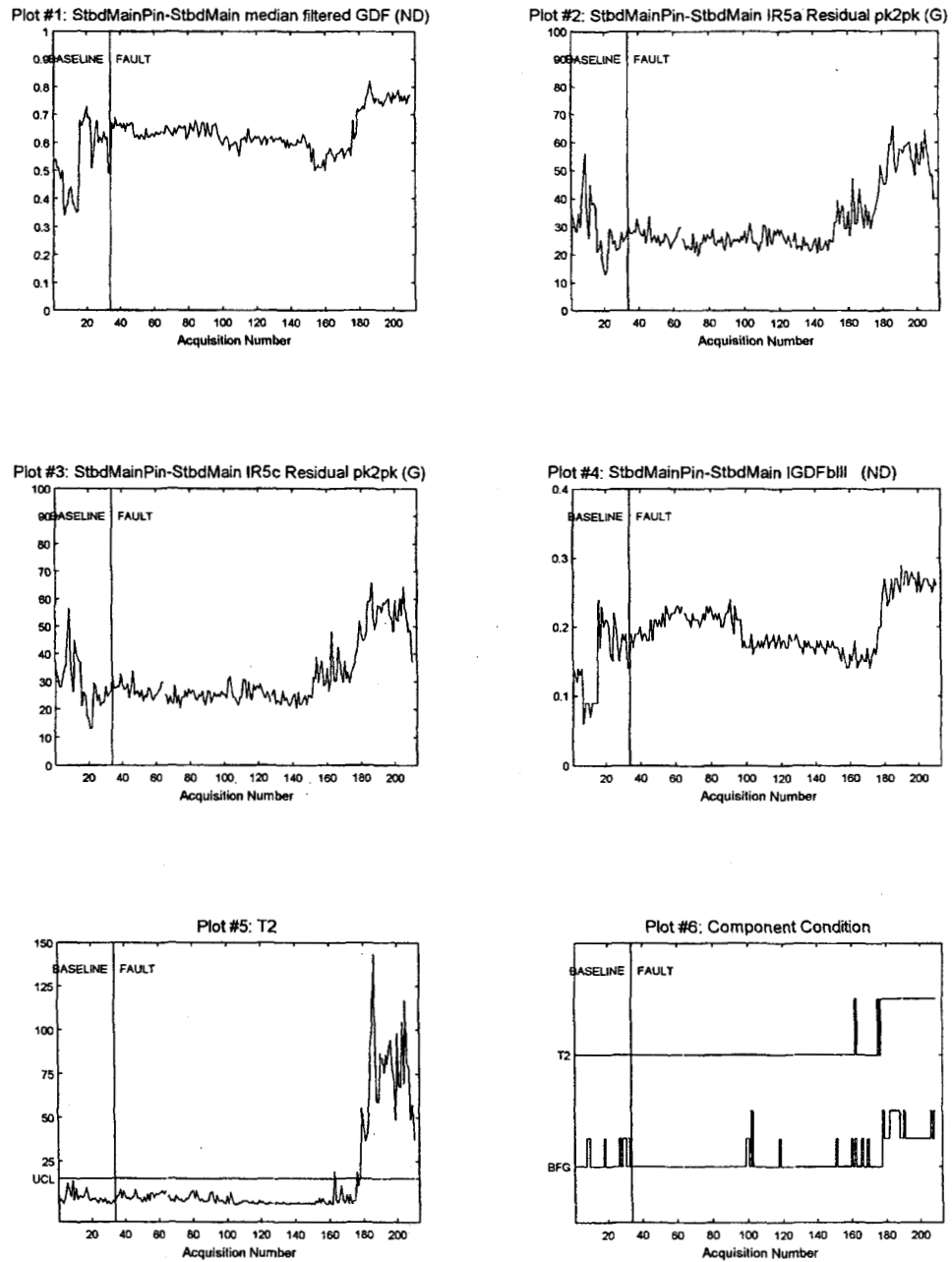
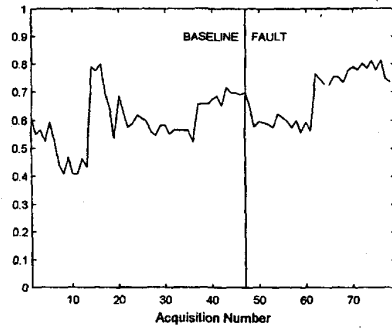
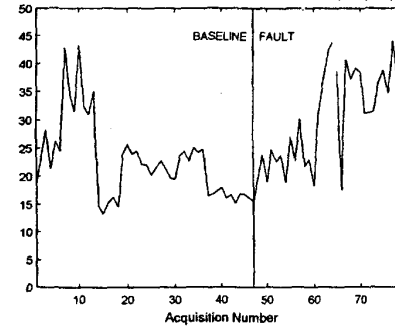


Figure 2. Main Module Starboard Input Pinion Crack Propagation Data: High Torque Indicators Selected from Starboard Main Accelerometer for Max Indicator Δ Correlation from Baseline to Fault Data.

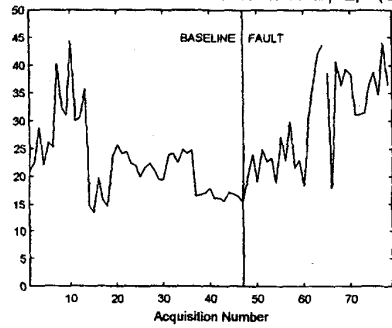
Plot #1: StbdMainPin-StbdMain median filtered GDF (ND)



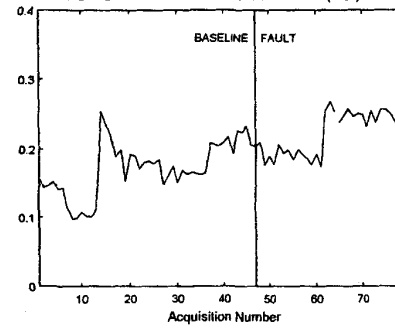
Plot #2: StbdMainPin-StbdMain IR5a Residual pk2pk (G)



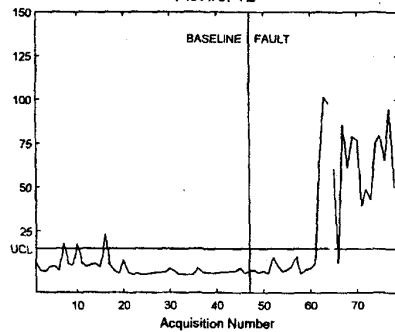
Plot #3: StbdMainPin-StbdMain IR5c Residual pk2pk (G)



Plot #4: StbdMainPin-StbdMain IGDFbIII (ND)



Plot #5: T2



Plot #6: Component Condition

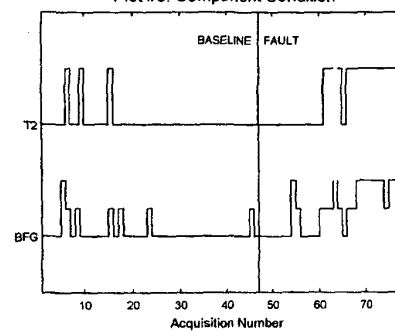


Figure 3. Main Module Starboard Input Pinion Crack Propagation Data: Low Torque Indicators Selected from Starboard Main Accelerometer for Max Indicator Δ Correlation from Baseline to Fault Data.

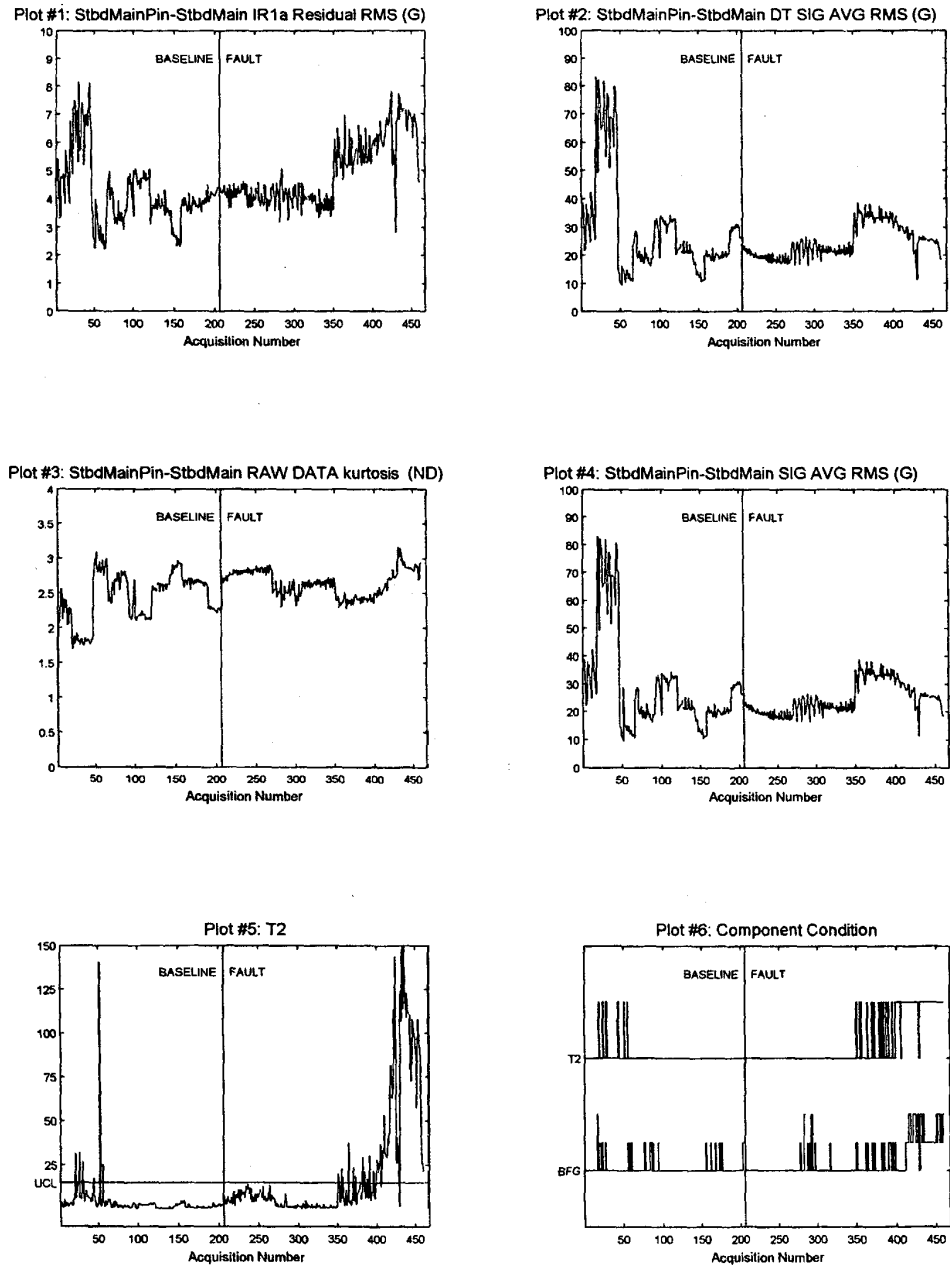


Figure 4. Main Module Starboard Input Pinion Crack Propagation Data: All Torque Indicators Selected from Starboard Main Accelerometer for Max Indicator Anti-Correlation in Baseline Data.

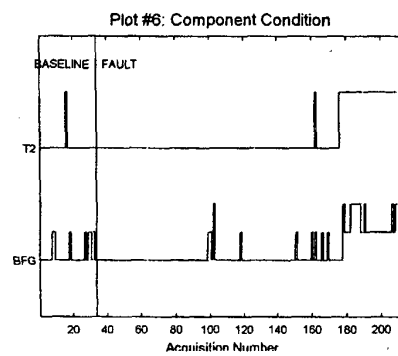
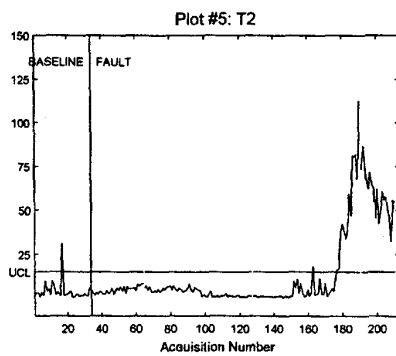
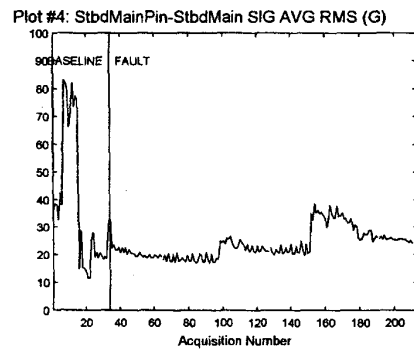
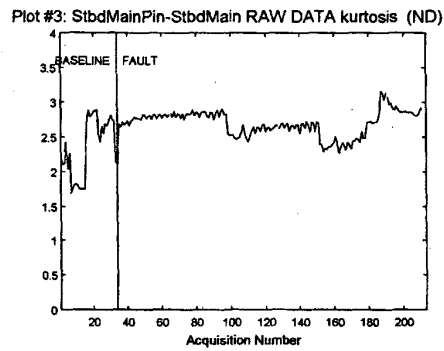
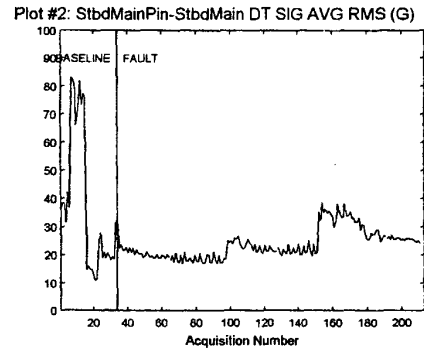
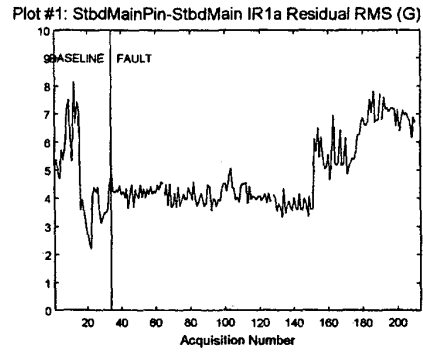
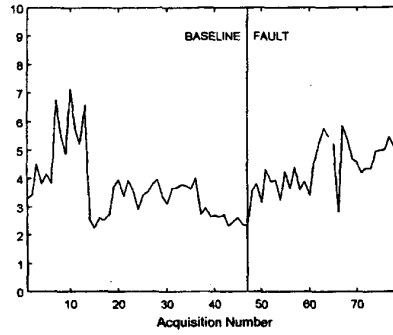
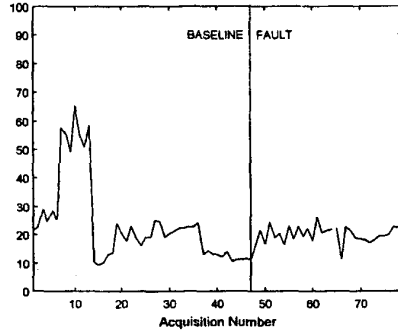


Figure 5. Main Module Starboard Input Pinion Crack Propagation Data: High Torque Indicators Selected from Starboard Main Accelerometer for Max Indicator Anti-Correlation in Baseline Data.

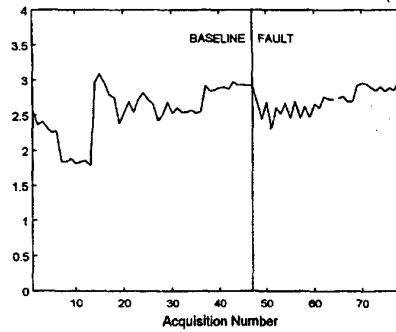
Plot #1: StbdMainPin-StbdMain IR1a Residual RMS (G)



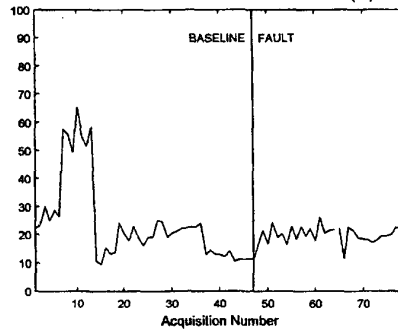
Plot #2: StbdMainPin-StbdMain DT SIG AVG RMS (G)



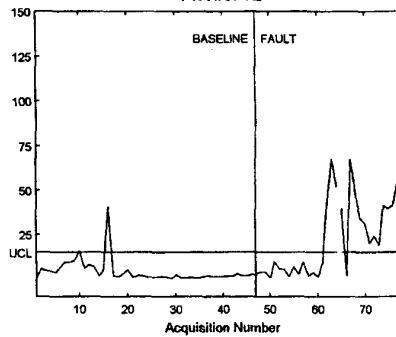
Plot #3: StbdMainPin-StbdMain RAW DATA kurtosis (ND)



Plot #4: StbdMainPin-StbdMain SIG AVG RMS (G)



Plot #5: T2



Plot #6: Component Condition

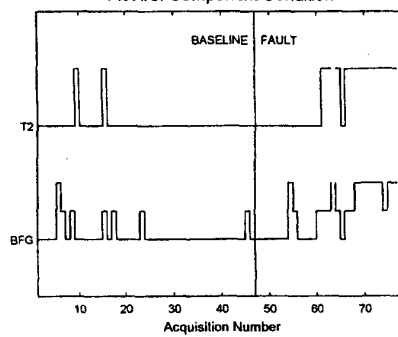
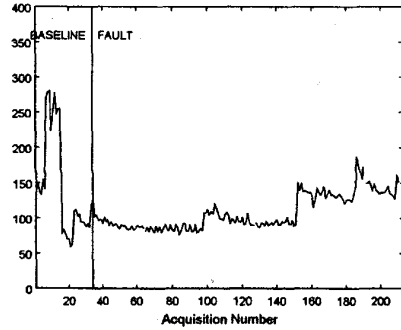
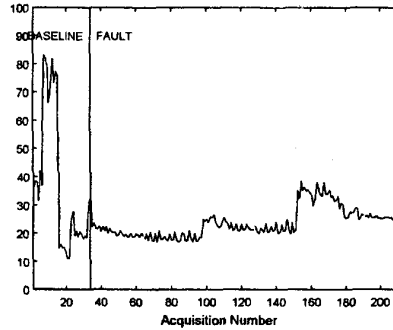


Figure 6. Main Module Starboard Input Pinion Crack Propagation Data: Low Torque Indicators Selected from Starboard Main Accelerometer for Max Indicator Anti-Correlation in Baseline Data.

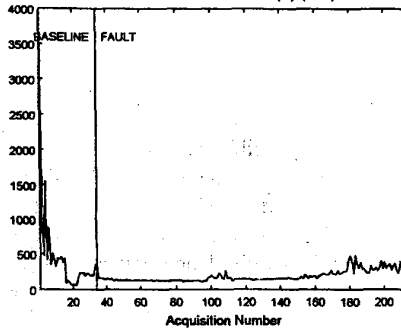
Plot #1: StbdMainPin-StbdMain DT SIG AVG pk2pk (G)



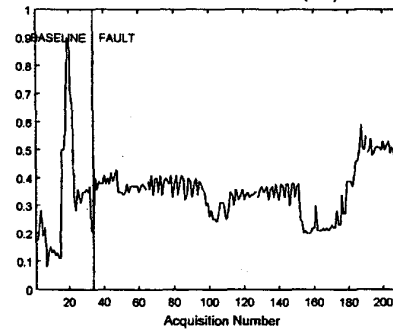
Plot #2: StbdMainPin-StbdMain DT SIG AVG RMS (G)



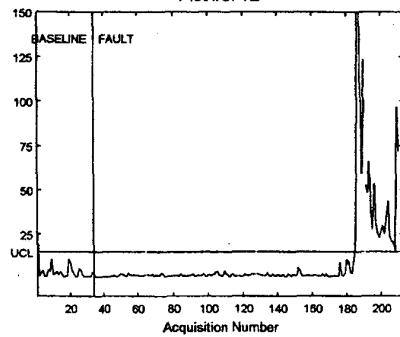
Plot #3: StbdMainPin-StbdMain G2(3) (ND)



Plot #4: StbdMainPin-StbdMain IGDFa (ND)



Plot #5: T2



Plot #6: Component Condition

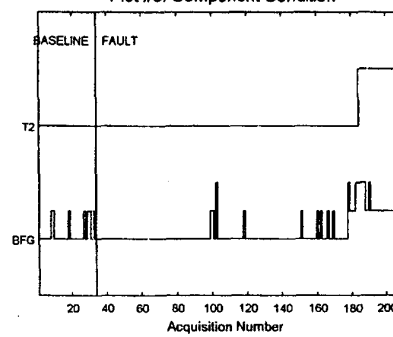


Figure 7. Main Module Starboard Input Pinion Crack Propagation Data: High Torque Indicators Selected from Starboard Main Accelerometer That Do Not Exceed Individual Alarm Thresholds.

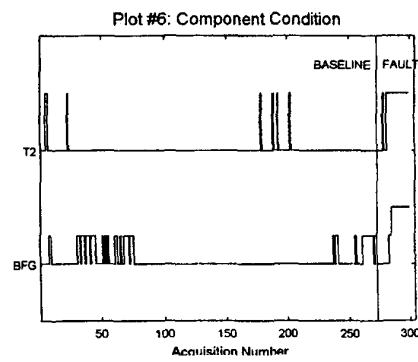
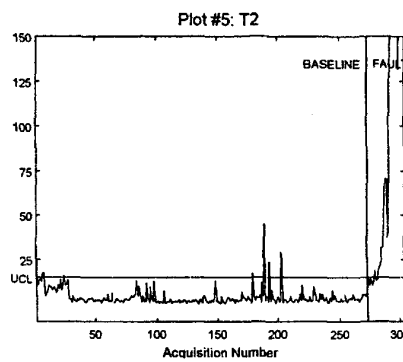
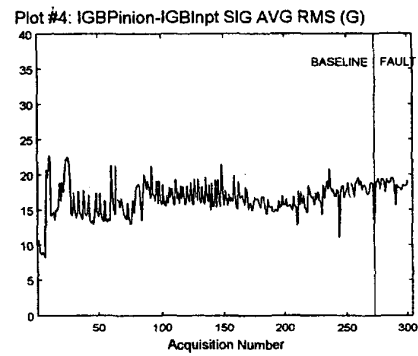
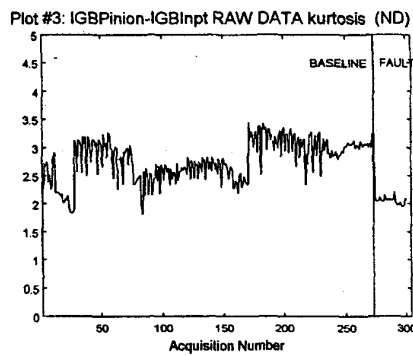
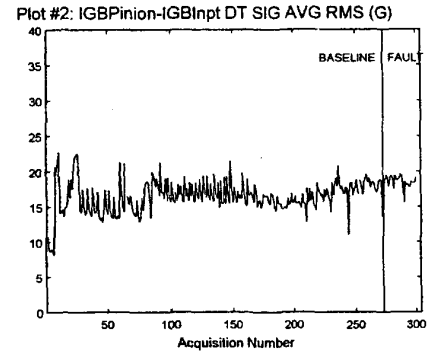
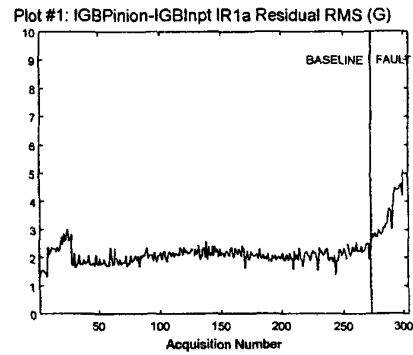


Figure 8. Intermediate Gearbox Input Pinion Crack Propagation Data: High Torque Indicators Selected from Main Module Starboard Input Pinion Crack Propagation Data.

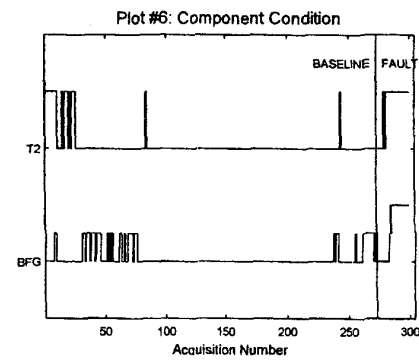
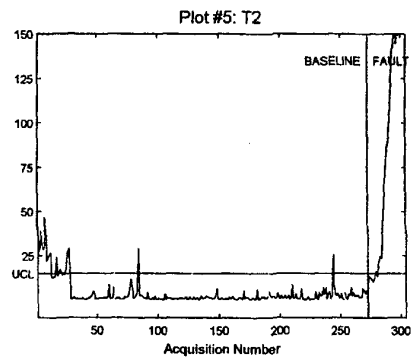
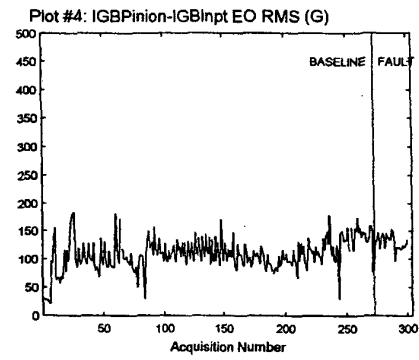
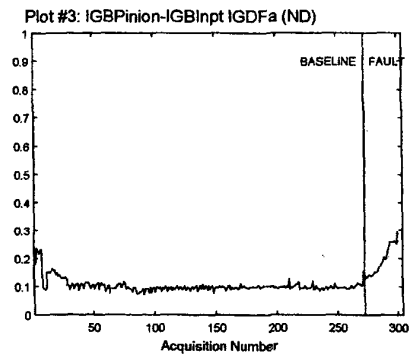
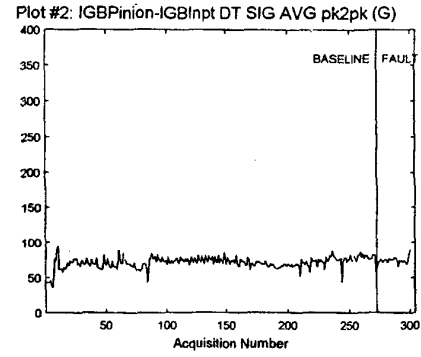
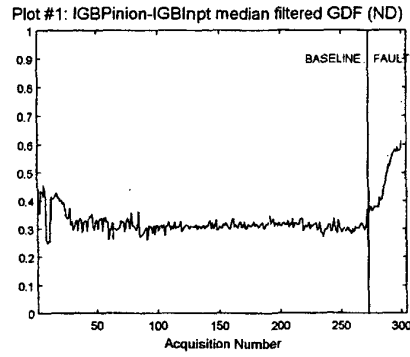


Figure 9. Intermediate Gearbox Input Pinion Crack Propagation Data: High Torque Indicators Selected from IGB Input Accelerometer for Max Indicator Anti-Correlation in Baseline Data.

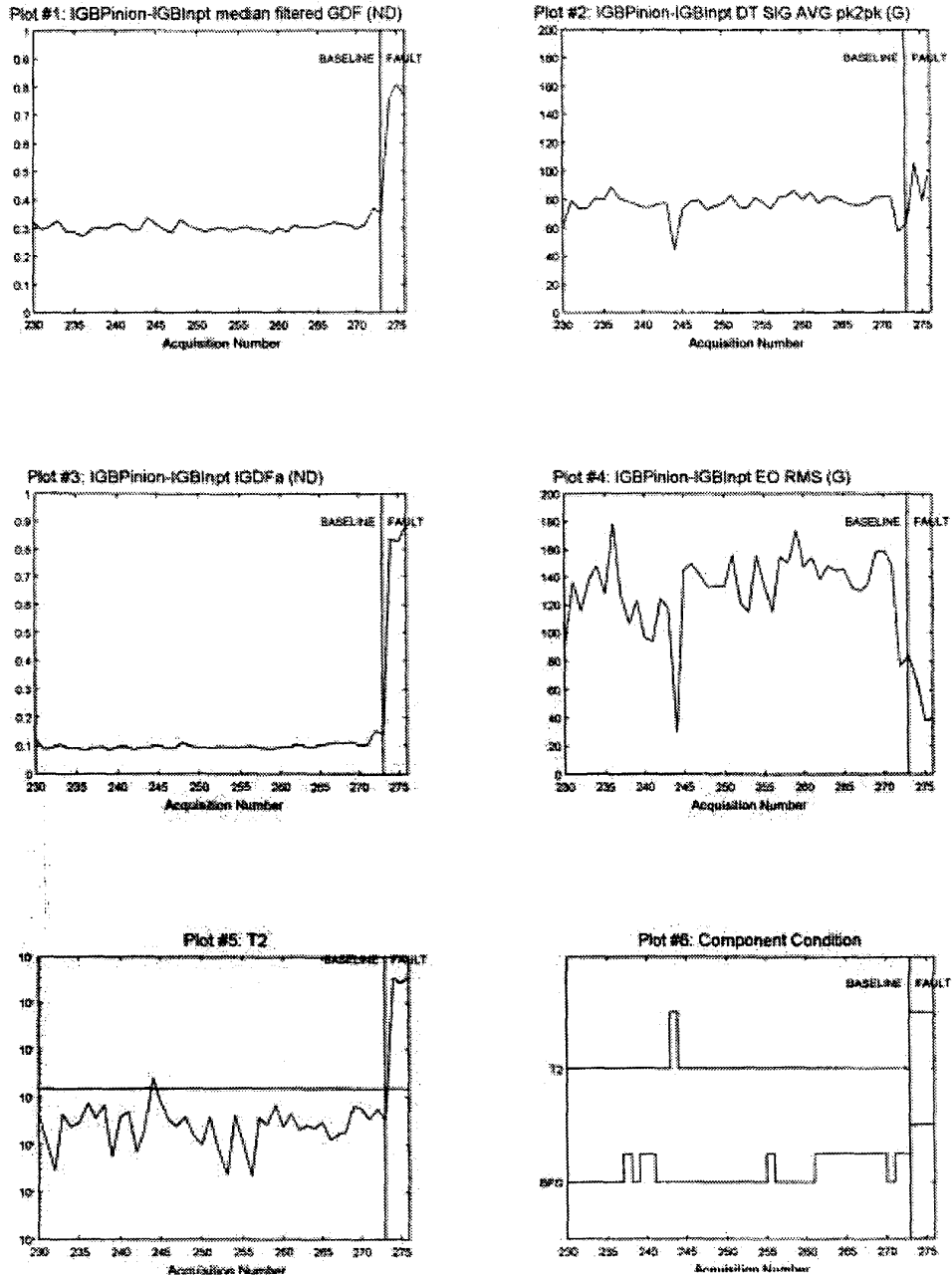
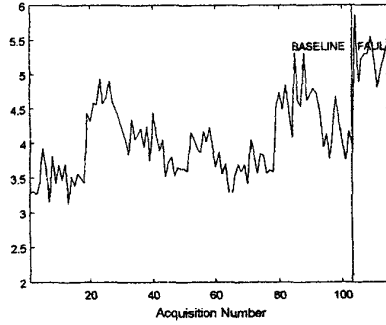


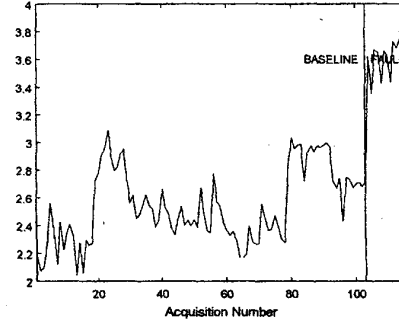
Figure 10. Intermediate Gearbox Input Pinion Crack Propagation Data: High Torque Indicators Selected from Intermediate Gearbox Input Pinion 1/3 Tooth Data.

Appendix B: Results of T2 Bearing Analysis

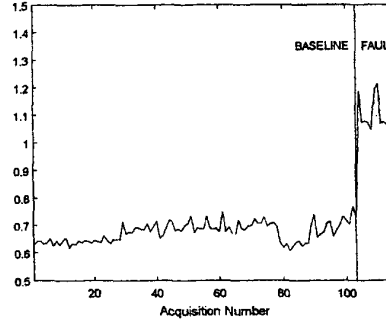
Plot #1: StbdMainPinRoller-StbdMain Raw Crest Factor



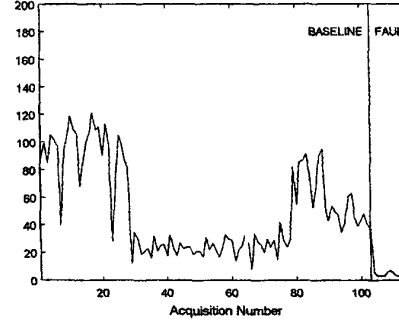
Plot #2: StbdMainPinRoller-StbdMain Raw Kurtosis



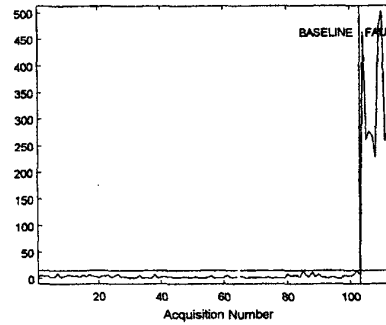
Plot #3: StbdMainPinRoller-StbdMain Enveloped Skewness



Plot #4: StbdMainPinRoller-StbdMain Number of Peaks



Plot #5: T2



Plot #6: Component Condition

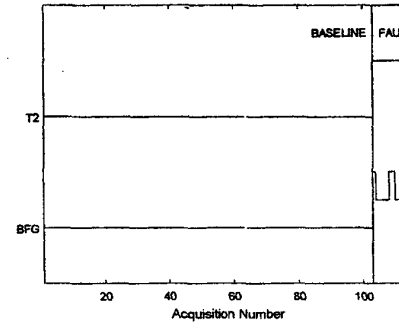


Figure 11. Main Module Starboard Input Pinion Roller Bearing Integral Race Spall Data: All Torque Indicator Suite 1 Selected from Starboard Main Accelerometer for Max Indicator Anti-Correlation in Baseline Data.

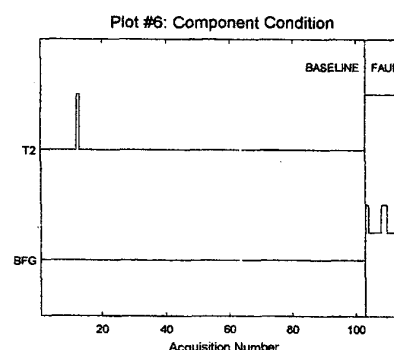
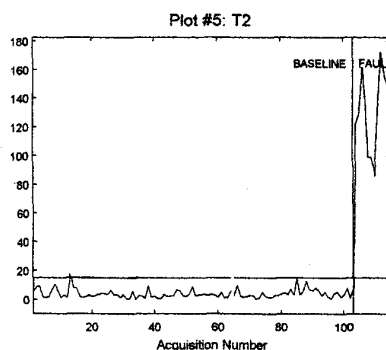
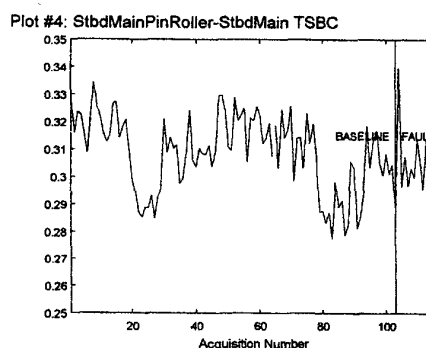
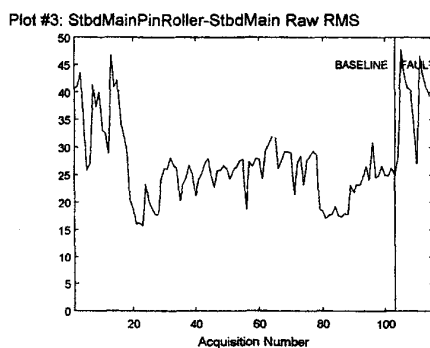
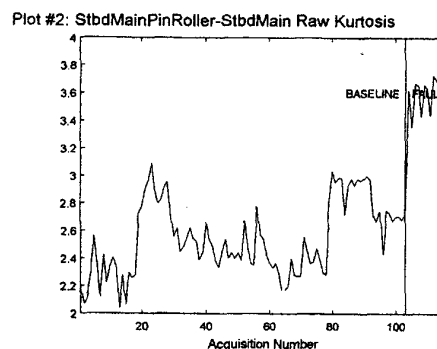
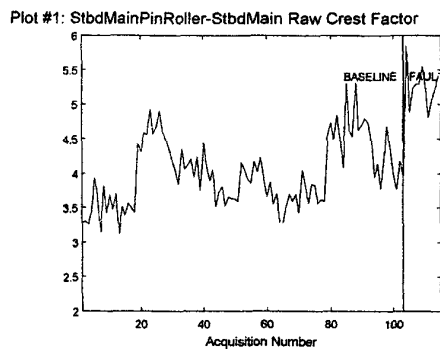
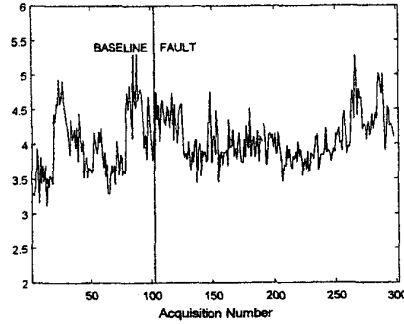
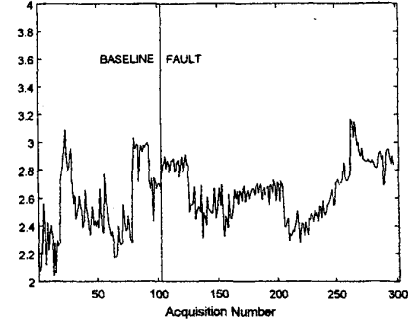


Figure 12. Main Module Starboard Input Pinion Roller Bearing Integral Race Spall Data: All Torque Indicator Suite 2 Selected from Starboard Main Accelerometer for Max Indicator Anti-Correlation in Baseline Data.

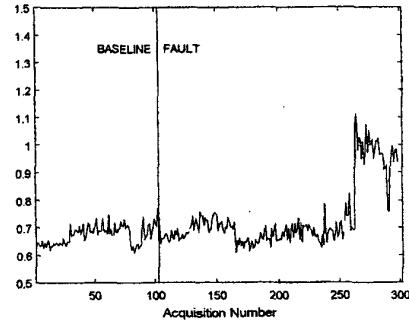
Plot #1: StbdMainPinRoller-StbdMain Raw Crest Factor



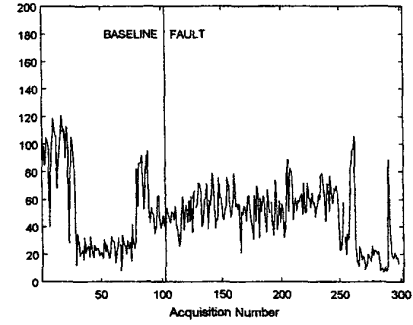
Plot #2: StbdMainPinRoller-StbdMain Raw Kurtosis



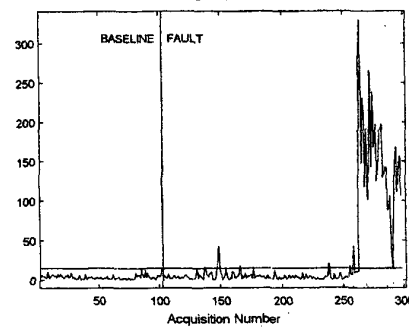
Plot #3: StbdMainPinRoller-StbdMain Enveloped Skewness



Plot #4: StbdMainPinRoller-StbdMain Number of Peaks



Plot #5: T2



Plot #6: Component Condition

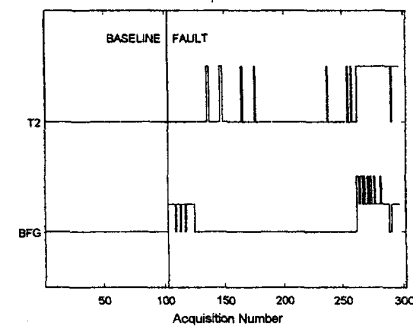
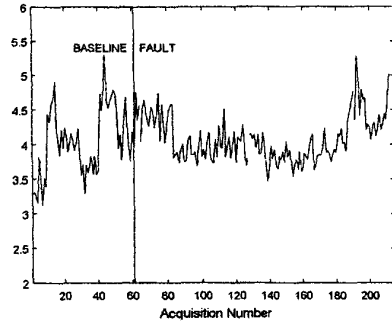
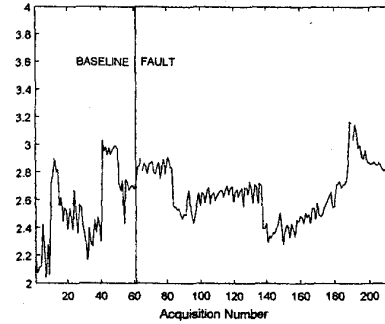


Figure 13. Main Module Starboard Input Pinion Roller Bearing Integral Race Spall Data: All Torque Indicator Suite 1 Selected from Starboard Main Accelerometer for Max Indicator Anti-Correlation in Baseline Data.

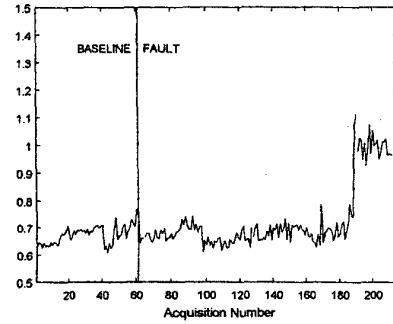
Plot #1: StbdMainPinRoller-StbdMain Raw Crest Factor



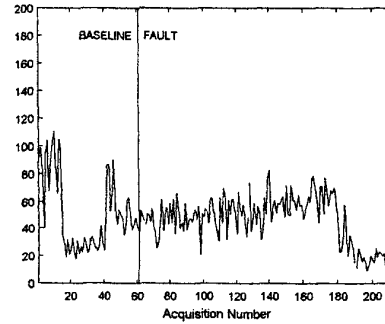
Plot #2: StbdMainPinRoller-StbdMain Raw Kurtosis



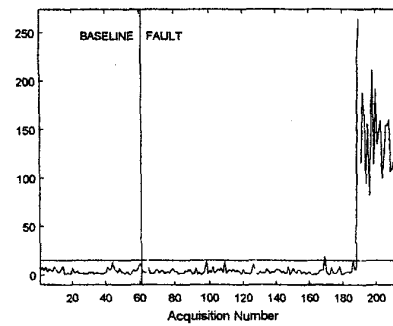
Plot #3: StbdMainPinRoller-StbdMain Enveloped Skewness



Plot #4: StbdMainPinRoller-StbdMain Number of Peaks



Plot #5: T2



Plot #6: Component Condition

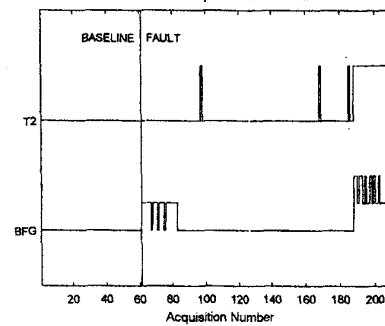
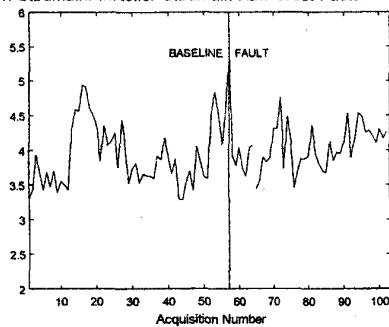
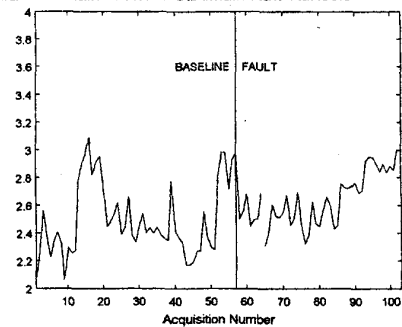


Figure 14. Main Module Starboard Input Pinion Roller Bearing Integral Race Spall Data: High Torque Indicator Suite 1 Selected from Starboard Main Accelerometer for Max Indicator Anti-Correlation in Baseline Data.

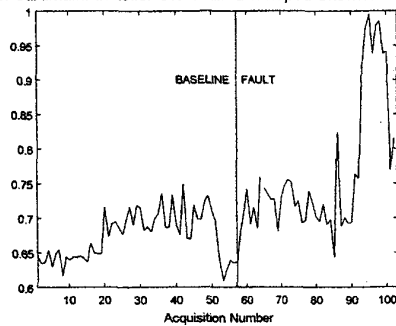
Plot #1: StbdMainPinRoller-StbdMain Raw Crest Factor



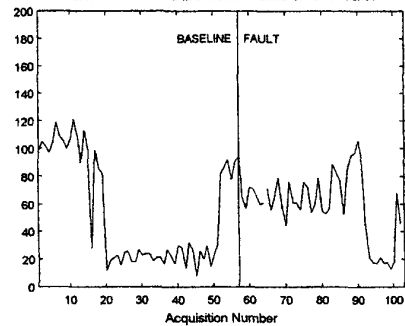
Plot #2: StbdMainPinRoller-StbdMain Raw Kurtosis



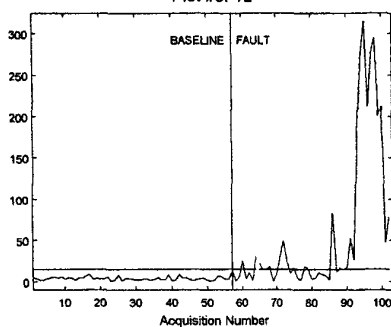
Plot #3: StbdMainPinRoller-StbdMain Enveloped Skewness



Plot #4: StbdMainPinRoller-StbdMain Number of Peaks



Plot #5: T2



Plot #6: Component Condition

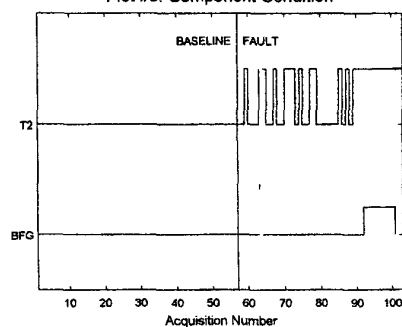


Figure 15. Main Module Starboard Input Pinion Roller Bearing Integral Race Spall Data: Low Torque Indicator Suite 1 Selected from Starboard Main Accelerometer for Max Indicator Anti-Correlation in Baseline Data.

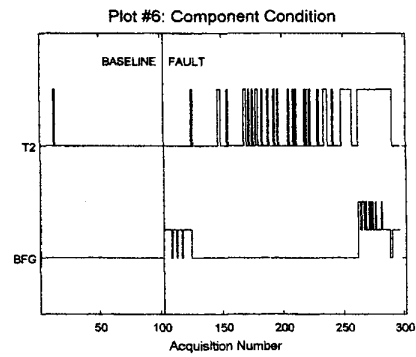
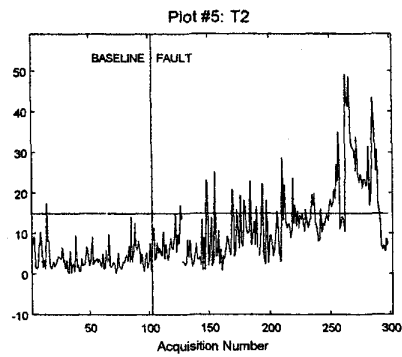
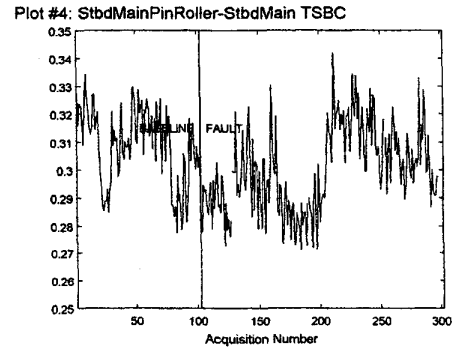
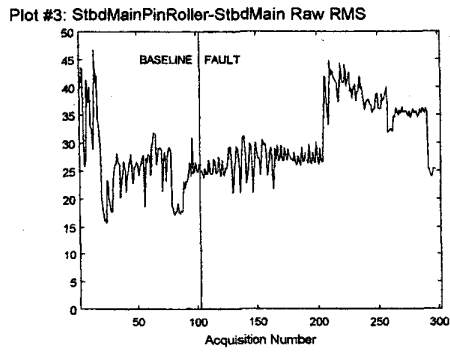
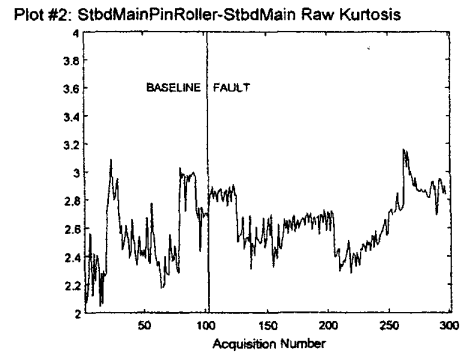
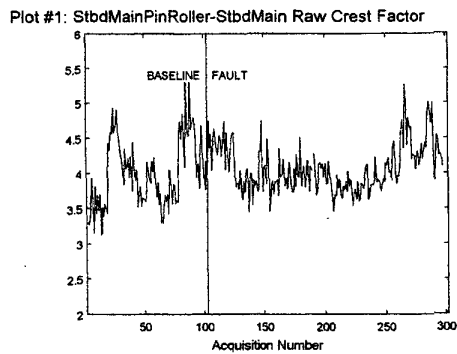
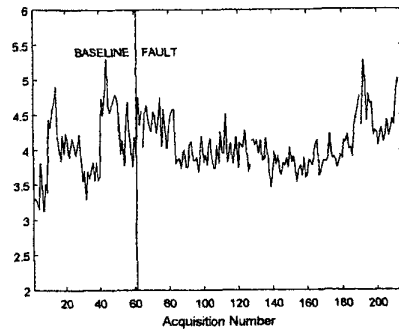
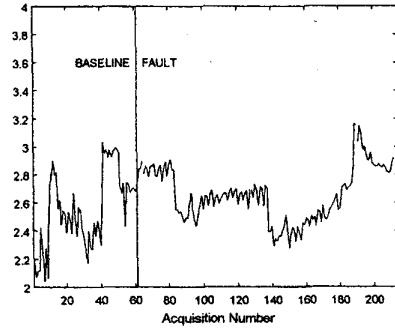


Figure 16. Main Module Starboard Input Pinion Roller Bearing Integral Race Spall Data: All Torque Indicator Suite 2 Selected from Starboard Main Accelerometer for Max Indicator Anti-Correlation in Baseline Data.

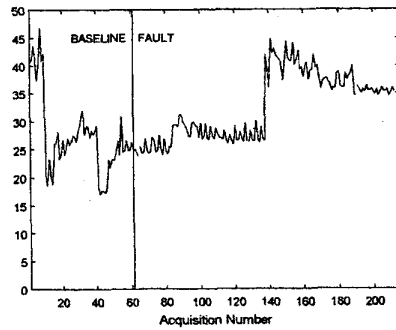
Plot #1: StbdMainPinRoller-StbdMain Raw Crest Factor



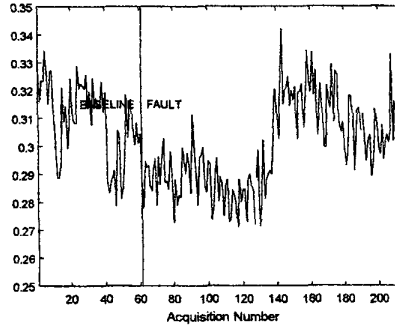
Plot #2: StbdMainPinRoller-StbdMain Raw Kurtosis



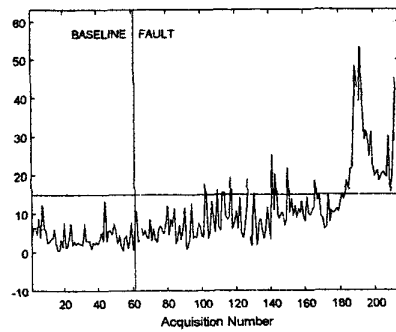
Plot #3: StbdMainPinRoller-StbdMain Raw RMS



Plot #4: StbdMainPinRoller-StbdMain TSBC



Plot #5: T2



Plot #6: Component Condition

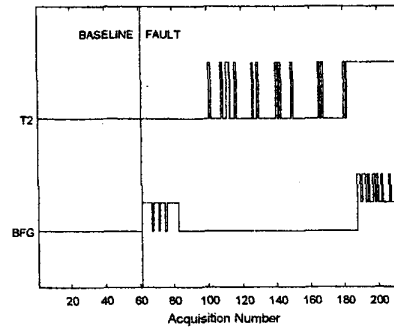
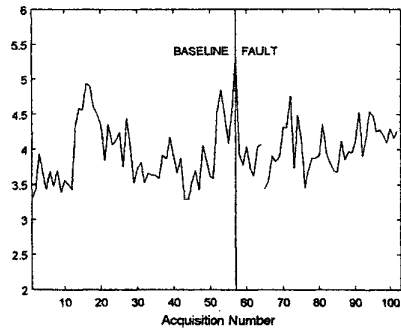
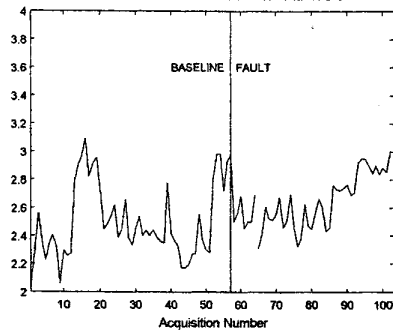


Figure 17. Main Module Starboard Input Pinion Roller Bearing Integral Race Spall Data: High Torque Indicator Suite 2 Selected from Starboard Main Accelerometer for Max Indicator Anti-Correlation in Baseline Data.

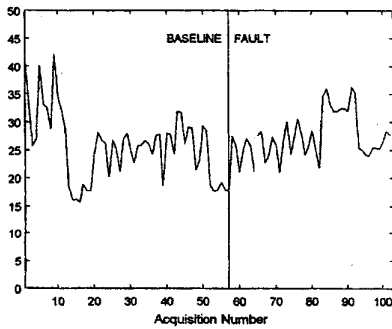
Plot #1: StbdMainPinRoller-StbdMain Raw Crest Factor



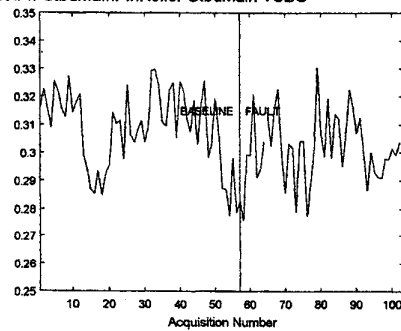
Plot #2: StbdMainPinRoller-StbdMain Raw Kurtosis



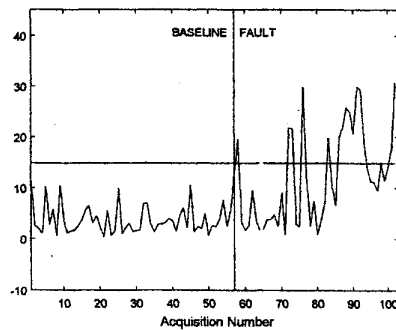
Plot #3: StbdMainPinRoller-StbdMain Raw RMS



Plot #4: StbdMainPinRoller-StbdMain TSBC



Plot #5: T2



Plot #6: Component Condition

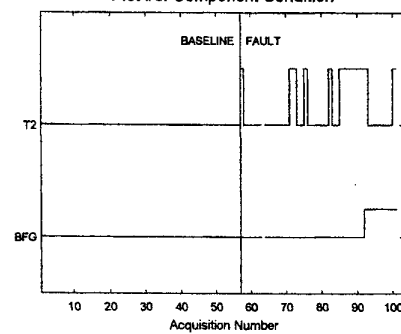


Figure 18. Main Module Starboard Input Pinion Roller Bearing Integral Race Spall Data: Low Torque Indicator Suite 2 Selected from Starboard Main Accelerometer for Max Indicator Anti-Correlation in Baseline Data.